

# Predicting flow resistance in rough-bed rivers from topographic roughness: Review and open questions

Robert I. Ferguson<sup>1</sup>  | Richard J. Hardy<sup>1</sup> | Rebecca A. Hodge<sup>1</sup>  |  
Robert C. Houseago<sup>1,2</sup>  | Elowyn M. Yager<sup>3</sup>  | Taís N. Yamasaki<sup>1</sup>

<sup>1</sup>Department of Geography, Durham University, Durham, UK

<sup>2</sup>Now at Department of Geography and Environment, Loughborough University, Loughborough, UK

<sup>3</sup>Center for Ecohydraulics Research, Department of Civil & Environmental Engineering, University of Idaho, Boise, Idaho, USA

## Correspondence

Robert I. Ferguson, Department of Geography, Durham University, Durham, UK.  
Email: [r.i.ferguson@durham.ac.uk](mailto:r.i.ferguson@durham.ac.uk)

## Funding information

Funding acknowledged from UKRI grant NE/W00125X/1.

## Abstract

Most ways of predicting flow resistance in shallow rivers with a partial or complete cover of coarse sediment use a bed-sediment grain diameter as a roughness length scale. However, beds with the same grain size distribution differ in roughness and flow resistance depending on how the larger grains are arranged, the nature of any bedforms and the possible complications of bedrock or rough banks. This has led to interest in predicting flow resistance using metrics of the topographic roughness of the bed. Some researchers have used the standard deviation of bed elevation as a roughness length scale. An alternative for channels containing boulders is to regard the bed as an array of large roughness elements. Fluvial research to date using these two approaches is limited and inconclusive. We review potentially relevant findings from the much more extensive literature in boundary-layer meteorology and various branches of engineering and note links between the distribution-statistics and element-array approaches. The skewness of the elevation distribution is widely seen as important but it is unclear how best to use it for flow prediction. Other open questions include the scale dependence of topographic metrics, and what type of flow resistance equation to use them in. Calibration and testing of new prediction methods require flow data from reaches with known roughness statistics. This need should be met partly by measurements at field sites or in flume models of them, but also by flume experiments and numerical simulations using synthetic roughness.

## 1 | INTRODUCTION

Most low-order stream channels in mountains and uplands, and some larger rivers that traverse mountains or emerge from them, have beds that are much rougher than those usually found in lowland streams and rivers. The dominant surface sediment is coarse, possibly extending into the boulder size range, and any surface sand is restricted to small patches in sheltered locations. There may be exposed bedrock and it may have ribs and potholes. Flow is typically shallow relative to the vertical amplitude of bed irregularity, and the largest clasts may protrude above the water surface. We focus on channels of these types, and refer to them as rough-bed (Nikora et al., 2007), rather than coarse-bed, rivers to allow the inclusion of reaches with exposed bedrock. However, we narrow the scope slightly by assuming that any in-stream wood is too sparse to significantly affect the flow of the

stream. Figure 1 shows some contrasting examples of rough-bed streams and rivers.

At any given discharge, a rougher bed exerts more resistance to flow, which is therefore deeper and slower than on a smoother bed with the same slope. Differences in flow resistance affect local flood risk and aquatic ecology, and a resistance-related parameter must be specified in many analytical and numerical models in geomorphology and hydrology as well as in various practical calculations. Standard equations for predicting reach-average velocity and discharge from depth and slope, or depth and velocity from discharge and slope, are much less reliable for shallow flows over rough beds than they are for deeper flows (Ferguson, 2022; Rickenmann & Recking, 2011). Most such equations quantify 'roughness' by a representative bed grain size. This is inappropriate in channels that lack significant sediment cover over bedrock and is less than optimal even in predominantly

This is an open access article under the terms of the [Creative Commons Attribution](https://creativecommons.org/licenses/by/4.0/) License, which permits use, distribution and reproduction in any medium, provided the original work is properly cited.

© 2024 The Author(s). *Earth Surface Processes and Landforms* published by John Wiley & Sons Ltd.

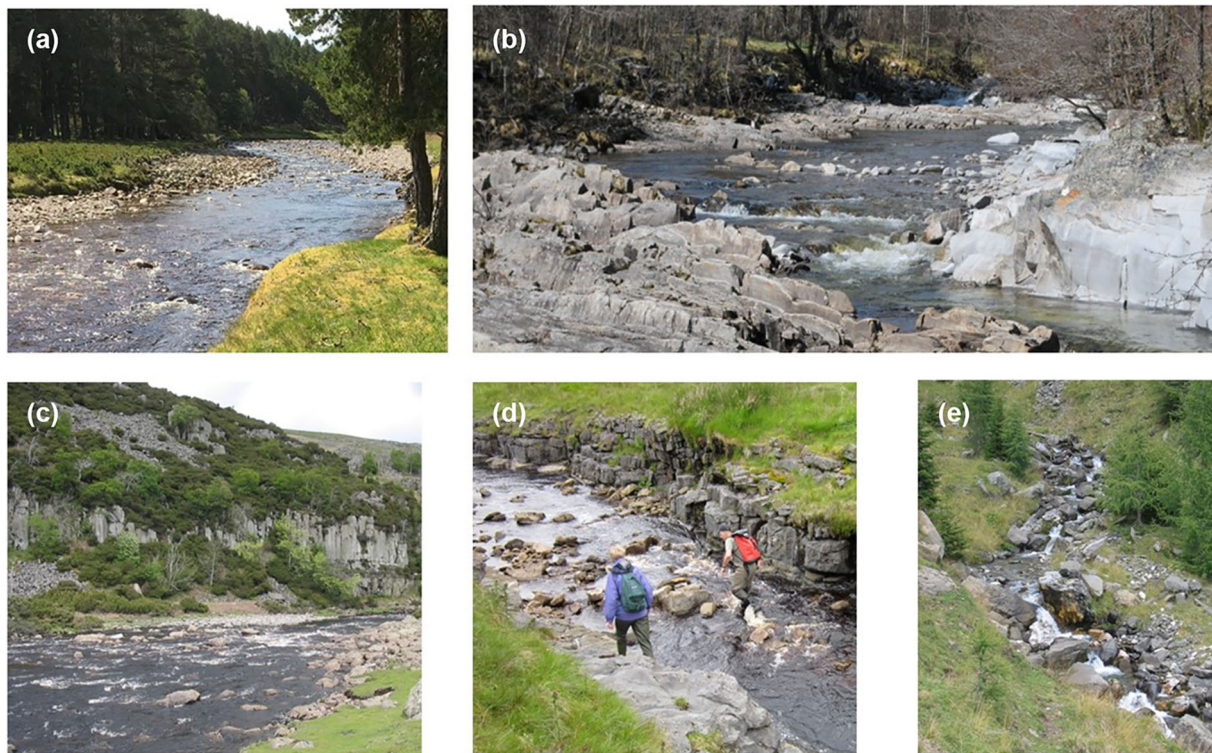


**FIGURE 1** Different types of rough-bed channel: (a) small gravel-bed river; (b) coarse sediment on tilted bedrock; (c) cobble-bed river with hillslope-derived boulders; (d) bedrock floor with plucked and collapsed blocks; (e) boulder steps and pools. (Author photographs.)

alluvial channels because the same coarse grain-size distribution can exert more or less resistance to flow depending on how the grains are arranged. In alluvial channels with coarse beds, the grain-size distribution is always wide and the larger grains usually protrude above the general bed level, thus generating form drag. This is the rationale for using a percentile from the coarse tail of the distribution ( $D_{84}$  or  $D_{90}$ ), rather than the median ( $D_{50}$ ), to predict flow resistance. But differences still remain between tightly-imbricated and more loosely-packed beds, even before considering bedforms ranging in size from pebble clusters (Brayshaw, Frostick, & Reid, 1983; Hassan & Reid, 1990) and stone cells (Church, Hassan, & Wolcott, 1998) to steps (Zimmerman, 2010) and bars (Parker & Peterson, 1980). The recognition that a grain size percentile can never fully characterise bed roughness has led many researchers to suggest that it is better in principle to use metrics of the bed topography itself (Furbish, 1987; Gomez, 1993; Lane, 2005; Smart et al., 2004; Smart, Duncan, & Walsh, 2002).

This state-of-science review is about ways to quantify topographic irregularity for the purpose of predicting flow in rough-bed rivers. It is written as a contribution to geomorphology, not fluid mechanics, but we argue that there are lessons to be learned from research in disciplines other than geomorphology. The effects of surface roughness on near-boundary flow have been investigated quite extensively in contexts that range from aeronautics and air flow around buildings to soil erosion and drag on ships' hulls. There have been several reviews of the state of knowledge in these contexts, most recently by Chung et al. (2021). Most of these other boundary layers lack a free surface but they still involve turbulent flow within and above a roughness layer, and they have been investigated with the same methods that fluvial geomorphologists use: analytical

models, field and laboratory measurements, curve fitting and computational fluid dynamics (CFD) modelling.

Our aim is to synthesise what has been discovered about the relation of flow resistance to surface roughness in various kinds of fully rough turbulent boundary layers, and thus to identify some new ideas about predicting bulk flow resistance in rough-bed rivers. In so doing we also identify several open questions. The remainder of the paper is in six parts. Section 2 considers the distinctive features of shallow flow over rough river beds. Section 3 summarises research by geomorphologists and hydraulic engineers on ways to measure and analyse the topographic roughness of river beds. Section 4 is about predicting flow resistance from statistical moments of topographic roughness, and is mainly about the manufactured surfaces of interest to various branches of engineering. In Section 5 we consider an alternative approach which focuses on the drag exerted by individual large roughness elements, whether in rivers or other contexts such as urban meteorology and aeolian geomorphology. In Section 6 we identify some links between the moment-statistics and obstacle-array approaches and what they imply about the near-equivalence of alternative metrics. Finally, Section 7 draws some tentative conclusions and identifies several open questions and pointers for future research.

## 2 | SHALLOW OPEN-CHANNEL FLOW

In open-channel flow, as in other flows that contain turbulent boundary layers, the vertical profile of time-averaged velocity is often assumed to be logarithmic within some, maybe most, of the range of height above the bed. This logarithmic part of the profile, if it exists, is described by

$$u/u^* = (1/\kappa) \ln(y/y_0) = (1/\kappa) \ln(30y/k_s) \quad (1)$$

where  $u$  is the velocity at height  $y$ ,  $u^*$  denotes shear velocity,  $\kappa$  is the von Kármán constant ( $\sim 0.4$ ),  $y_0$  is determined by fitting Equation (1) to velocity measurements at different heights and  $k_s = 30y_0$  is the equivalent sand roughness. The latter gets its name from the experimental finding that  $y_0/D \sim 30$  for pipes roughened with sand of diameter  $D$  (Nikuradse, 1933; Schlichting, 1936). The shear velocity is related to bulk flow properties by  $u^* = (\tau/\rho)^{1/2} = (gRS)^{1/2}$  where  $g$ ,  $R$ ,  $S$ ,  $\tau$  and  $\rho$  are the gravity acceleration, hydraulic radius, energy slope, mean bed shear stress and fluid density, respectively. In wide channels,  $R$  is almost the same as the mean flow depth  $h$ , and in uniform flow, the energy slope is the same as the water surface slope and mean bed slope.

There may be some deviation from a logarithmic profile towards the water surface, and there certainly is within a near-bed roughness layer that extends from the lowest points in the bed to a short way above the highest points. As the flow becomes shallower relative to the amplitude of bed irregularity, the roughness layer makes up an increasing part of the total flow depth, with no logarithmic layer at all in the limit case of a river with emergent boulders. The distinctive feature of the roughness layer is that streamlines within it converge and diverge between, around and over bed irregularities, with some loss of momentum through form-induced drag. Within the roughness layer, the mixing length of turbulent eddies depends on the amplitude of bed roughness, rather than on flow depth as in the logarithmic layer (Lawrence, 1997; Wiberg & Smith, 1991). The effects of spatial variance in flow can be included by averaging the Navier–Stokes equations for conservation of mass and momentum not just over time but also spatially in a bed-parallel plane (e.g. Nikora et al., 2001, 2007; Raupach & Shaw, 1982). This approach implies that the double-averaged velocity profile within the roughness layer depends on how the proportion of the cross-section occupied by bed protrusions varies with height. On this basis, Nikora et al. (2004) proposed that the spatially-averaged vertical velocity profile will often be approximately constant, linear or exponential. Near-constant velocity is only likely with cylindrical roughness elements such as emergent vegetation, which we have excluded from consideration.

In most engineering and meteorological contexts the boundary above which flow occurs is well defined. This is also true of exposed bedrock in rivers, but not of coarse alluvial beds where the definition of bed level (and thus also flow depth) is less clear. Unless the void spaces in the coarse matrix are completely filled with fine sediment there is some subsurface flow, and it may be substantial at topographic high points such as riffles (e.g. Tonina & Buffington, 2007). Possible definitions of bed level are the mean elevation derived from a DEM (e.g. Smart, Duncan, & Walsh, 2002) or the height below which sediment and water each occupy 50% of the cross-section (Deal, 2022). In both cases, there is some flow below this level, which cannot therefore be  $y = 0$  in Equation (1). Ways round this are to replace  $y$  by  $y-d$  in Equation (1), where  $d$  is known as the displacement height, or to use a modified log profile derived by assuming that the mixing length is a combination of roughness amplitude and flow depth (Lamb, Brun, & Fuller, 2017).

Faced with this complexity, simple methods of predicting the flow resistance exerted by rough beds are either purely empirical or involve physical assumptions and some calibration. As noted in reviews by

Powell (2014) and Ferguson (2022), almost all such methods can be viewed as ways of predicting the Chézy–Darcy–Weisbach friction factor  $f$ , which is defined by

$$(8/f)^{1/2} = v/u^* = v/(gRS)^{1/2} \approx v/(ghS)^{1/2} \quad (2)$$

where  $v$  denotes the reach-averaged mean velocity. The most widely-used flow resistance equations all have the form

$$(8/f)^{1/2} = f_n(R/D \text{ or } h/D) \quad (3)$$

where  $f_n$  is a monotonic function and  $D$  is a representative river-bed grain diameter used as a roughness length scale. The ratio  $R/D$  or  $h/D$  is termed relative submergence.

If the logarithmic velocity profile of Equation (1) holds over the full flow depth in a wide channel, integrating it leads to a logarithmic flow resistance law:

$$(8/f)^{1/2} = v/u^* = (1/\kappa) \ln(30h/\exp(1)k_s) \approx 2.5 \ln(11h/k_s) \quad (4)$$

(Keulegan, 1938). By analogy with Nikuradse's work,  $k_s$  should equal the median grain diameter ( $D_{50}$ ) in the ideal case of a plane bed of well-sorted sediment. In shallow flows the assumption of a logarithmic velocity profile is incorrect, but Equation (4) still gives a fairly good fit to bulk flow measurements in gravel- and boulder-bed rivers if  $k_s$  is increased to a multiple of  $D_{84}$  or  $D_{90}$  to account for sources of resistance additional to the skin friction of uniform sediment (e.g. Bray, 1980; Ferguson, 2007; Hey, 1979).

Other relative-submergence flow resistance equations that use a grain diameter as the roughness height include the Manning equation in the form  $(8/f)^{1/2} \propto (R/D)^{1/6}$  (e.g. Parker, 1991), empirical logarithmic relations not based on Equation (4) (e.g. Bathurst, 1985) and empirical power laws with exponents greater than  $1/6$  (e.g. Bathurst, 2002; Griffiths, 1981). Another is the variable-power equation proposed by Ferguson (2007) which has asymptotic exponents of  $1/6$  for deep flows and  $1$  for very shallow flows. The dimensionally consistent hydraulic geometry relations proposed by Aberle and Smart (2003) and Rickenmann and Recking (2011) can also be expressed in terms of relative submergence.

Analyses of extensive compilations of bulk flow measurements in rivers with coarse alluvial beds have shown that, whilst some resistance equations reproduce overall trends well, predictions of velocity (and thus discharge) from  $R/D_{84}$  or  $h/D_{84}$  at individual sites can still be incorrect by more than 50% (Ferguson, 2022; Rickenmann & Recking, 2011). Errors in predicting depth from discharge are similarly large. As can be seen in Figure 2, large prediction errors are particularly common in shallow flows in which the roughness layer occupies a significant part of the total depth, as is usual in rough-bed rivers. One reason for incorrect predictions is measurement error, particularly in channels containing boulders where grain-size sampling is difficult, cross-sections are difficult to survey accurately and mean velocity cannot be measured accurately by current meter. But the fundamental source of scatter in Figure 2 is the point we have already stressed: channels with the same surface grain-size distribution can differ in roughness and flow resistance according to grain arrangement and the presence or absence of larger-scale sources of resistance.

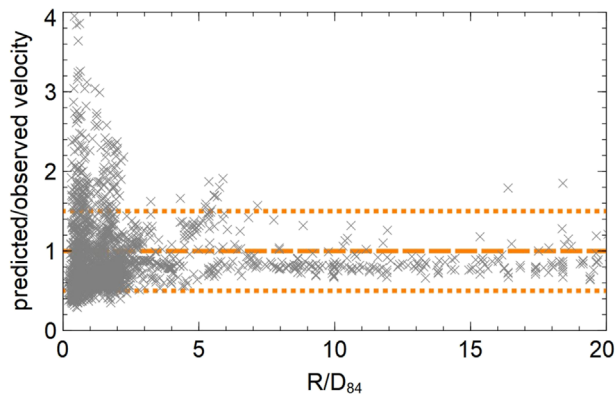


**FIGURE 2** Ratio of predicted to observed velocity in gravel- and boulder-bed channels. Data from Rickenmann and Recking (2011), predictions by the variable-power equation of Ferguson (2007). The dashed horizontal line indicates a perfect fit and the dotted lines are for errors of  $\pm 50\%$ .

Only a few attempts have been made to use directly-measured topographic roughness to predict flow resistance in rough-bed channels. Smart, Duncan, and Walsh (2002) and Aberle and Smart (2003) measured the standard deviation ( $\sigma_z$  hereafter) of local vertical departures from the general bed level and found that it outperformed  $D_{84}$  as a predictor of shallow flows over gravel in a flume. Yochum et al. (2012) and Chen et al. (2020) also found that velocity predictions using  $\sigma_z$  were generally superior to those using  $D_{84}$  in the same type of resistance equation. However, Nitsche et al. (2012) and Zimmerman (2010) found that  $D_{84}$  gave marginally better results than  $\sigma_z$  and Schneider et al. (2015) found no systematic difference.

Another way to use topographic metrics is to regard the bed as an array of large roughness elements protruding above a relatively smooth base and try to predict flow resistance from the size and other characteristics of the large elements. There have been some flume investigations on these lines using cubic blocks (e.g. Herbich & Shulits, 1964), hemispheres (e.g. Lawrence, 1997) or natural pebbles (e.g. Baiamonte & Ferro, 1997), and also a few field investigations (e.g. Bathurst, 1978; Wiener & Pasternak, 2022) and analytical models (e.g. Yager, Kirchner, & Dietrich, 2007). This strand of research has shown that flow resistance varies with the size, shape, spatial density and spatial arrangement of the large elements. Most attempts to use one or more of these variables to help predict flow resistance have involved a stress-partitioning approach or empirically-calibrated correction terms in a logarithmic resistance equation.

### 3 | QUANTIFICATION OF RIVER BED TOPOGRAPHY

Most flow-resistance equations were devised at a time when it was far easier to measure grain sizes by pebble count than to quantify topographic roughness. The latter could only be done by laborious manual methods, typically using a profiler consisting of closely-spaced point gauges along a beam (Ergenzinger, 1992; Furbish, 1987; Gomez, 1993). This enforced a trade-off between spatial resolution and spatial extent. Judd and Peterson (1969) measured the protrusion of the larger clasts in some boulder-bed streams in the US Rocky Mountains but did not summarise them by any kind of statistic; their

work on flow resistance focused instead on the spatial density of large roughness elements. Ergenzinger (1992) and Gomez (1993) devised metrics based on manual measurements of differences in elevation between adjacent grains, but their primary interest was in the effects of protrusion and pivot angles on grain entrainment. The use of topographic roughness to predict flow resistance became possible after technological developments in survey methods. Attention then turned to ways to summarise spatially-distributed roughness, and questions about scales of roughness.

#### 3.1 | New measurement technologies

Surveying by total station or differential GPS, and mapping by airborne LiDAR, allow much larger areas to be surveyed, but generally not at sufficient resolution to quantify grain-scale roughness. The necessary combination of high resolution and adequate spatial extent became available about 20 years ago with the development of short-range remote sensing methods based on laser scanning or photogrammetry. Terrestrial laser scanning (TLS) produces a 3-D point cloud which can be processed to create a 2.5-D digital elevation model (DEM) consisting of a surface elevation value ( $z$ ) at each location in a spatial ( $x$ - $y$ ) grid. The first application to river beds was by Smart et al. (2004) and Nikora and Walsh (2004), who investigated the topography of small ( $<1 \text{ m}^2$ ) parts of flume beds and gravel bars using a hand-held laser scanner. Within a few years, tripod-mounted scanners with a wide field of view became available, allowing geomorphologists to create DEMs of large gravel bars (e.g. Heritage & Milan, 2009; Hodge, Brasington, & Richards, 2009) and entire reaches (e.g. Brasington, Vericat, & Rychkov, 2012). Much of this early work was primarily concerned with establishing measurement protocols and efficient workflows for DEM creation. DEMs can also be created from digital images using photogrammetric methods (e.g. Butler, Lane, & Chandler, 1998), and structure-from-motion (SfM) processing allows cheap hand-held or drone-mounted cameras to be used (e.g. Fonstad et al., 2013; Westoby et al., 2012). Standard TLS and photogrammetric methods yield no information on submerged parts of river beds, so data collection is normally done in low-flow conditions with submerged areas either ignored or patched in using other methods.

Much of the geomorphological research using these various data collection techniques has been directed not at flow resistance but towards identifying individual grains and thereby estimating size distributions or mapping sedimentary facies (e.g. Heritage & Milan, 2009; Pearson et al., 2017; Vazquez-Tarrio et al., 2017; Woodget, Fyffe, & Carbonneau, 2018). Other work has focused primarily on the statistical properties of roughness, particularly the  $x$ - and  $y$ -direction spatial autocorrelation of the  $z$  values (e.g. Furbish, 1987; Nikora & Walsh, 2004; Penna et al., 2021; Robert, 1988).

#### 3.2 | The basic roughness metric and its limitations

Most applications using DEMs quantify roughness amplitude by the standard deviation of bed elevation:  $\sigma_z = [\sum z^2/n - \langle z \rangle^2]^{1/2}$  where  $\langle z \rangle$  denotes the mean value of  $z$  and  $n$  is the total number of locations at which  $z$  is known. Tribology and other branches of engineering have long used  $\sigma_z$  as a roughness metric (e.g. Hama, 1954), and

Smith (2014) mentions early applications to the surface roughness of soils (Kuipers, 1957) and sea ice (Banke & Smith, 1973). It was first used to predict flow resistance by Smart, Duncan, and Walsh (2002), who analysed laboriously-acquired DEMs of several river beds and employed  $\sigma_z$  in resistance predictions. Aberle and Smart (2003) compared  $\sigma_z$  and  $D_{84}$  as predictors of gravel-bed flow resistance in flume experiments, and Nitsche et al. (2012), Yochum et al. (2012) and Chen et al. (2020) made the same comparison for field sites using mid-channel long profiles surveyed by total station. As noted above, these investigators reached conflicting conclusions about the predictive value of  $\sigma_z$  in comparison with grain size. We show below that there are conceptual reasons why  $\sigma_z$  cannot be a perfect predictor, and that in engineering disciplines it is only the starting point in the search for correlations between flow resistance and the roughness of manufactured surfaces. One final point to note about  $\sigma_z$  is that its use extends to channels with exposed bedrock, in which the use of a grain size to predict flow resistance would be inappropriate (e.g. Finnegan, Sklar, & Fuller, 2007; Johnson, 2014).

Any high-resolution river-bed long profile or DEM contains quasi-random local irregularity – ‘roughness’ -- superimposed on some non-random overall morphology. In flumes, this is simply a constant downstream gradient, but in rivers there is often a long-wavelength periodic component (Adams, 2020). In sand-bed rivers, not considered here, this consists of ripples or dunes; in rough-bed channels, it could be a bar-pool-riffle sequence or alternating steps and pools. Quasi-periodic variation in roughness is also possible through the development of alternating finer and coarser patches (e.g. Iseya & Ikeda, 1987; Powell et al., 2016). How to define the boundary between larger-scale morphology and smaller-scale roughness is up to the analyst, and their choice will affect the value of  $\sigma_z$  that is obtained. In a plane-bed flume experiment, all that is necessary is to remove the overall longitudinal gradient of the bed, but that may not be adequate for a natural river channel. If  $\sigma_z$  is regarded as a metric of grain-scale roughness, some smoothing of the raw DEM or long profile is appropriate before calculating  $\sigma_z$  using the vertical residuals from the smoothed surface. It would not be sensible, though, to smooth out bed forms that generate significant flow resistance, notably boulder steps.

Smart et al. (2004) recommended the use of cubic (for a long profile) or bicubic (for a DEM) splines to smooth the surface between a sequence or grid of fixed points at which the elevation of all points within a certain radius is averaged, and Nitsche et al. (2012) used this procedure to smooth measured mid-channel long profiles in boulder-bed reaches. Chen et al. (2020), working with a large compilation of long profiles obtained from other researchers, relied on linear detrending but investigated the effect of further smoothing by a moving average of window length  $w$ . As might be anticipated, they found that  $\sigma_z$  decreased as  $w$  increased and profile irregularities were smoothed out. This method can be generalised to a gridded DEM: remove a linear trend, smooth the morphology using a sliding window of size  $w$  by  $w$ , then compute  $\sigma_z$  of the smoothed surface. A closely-related alternative is to use a high-pass filter to smooth the raw DEM before calculating  $\sigma_z$  (Buechel, Hodge, & Kenmare, 2022).

The above approaches smooth the overall morphology and then calculate  $\sigma_z$  from the residual variability. It is equally possible to proceed the other way round, as done for bedrock surfaces by Hodge and Hoey (2016). Their procedure was to remove a linear trend, compute  $\sigma_z$  multiple times for every position of a sliding

window of size  $w$  by  $w$ , then smooth (by simple averaging) the resulting matrix of estimates of  $\sigma_z$ . In this approach, the final estimate of  $\sigma_z$  increases with  $w$ . If adjacent elevations followed a first-order spatial autocorrelation, as envisaged by Furbish (1987) and Nikora, Goring, and Biggs (1998), the estimated value of  $\sigma_z$  would stabilise rapidly from small to moderate  $w$ , then be essentially constant. However, Penna et al. (2021) found that the value of  $\sigma_z$  in water-worked gravel in a flume did not stabilise until  $w$  was about 40 times  $D_{50}$ , and our experience when analysing DEMs from field sites is similar. This scale dependence of  $\sigma_z$  is one of several obstacles in the search for widely-applicable predictive equations for flow resistance using topographic roughness.

A second limitation of  $\sigma_z$  as a roughness metric becomes apparent if the frequency distribution of  $z$  is skewed. Skewness is quantified by the third-moment statistic

$$\gamma = \left[ \frac{\sum(z - \langle z \rangle)^3 / n}{\sigma_z^3} \right] \quad (5)$$

This statistic is nondimensional, has an open-ended range, and is positive for right-skewed distributions but negative for left-skewed distributions. Bertin and Friedrich (2014) and Penna et al. (2021) found near-Gaussian distributions for water-worked gravel beds in a flume, but others have found asymmetric distributions. Smart et al. (2004) obtained high-resolution DEMs of several small areas on gravel bars and found right-skewed distributions at every site. They attributed this to the partial infilling of surface hollows by finer grains. In flume experiments on armour development, both  $\sigma_z$  and skewness increase as finer grains are entrained or infiltrate into pore spaces and the protrusion of coarser grains increases (Powell et al., 2016).

Why skewed distributions are of concern with respect to flow resistance is apparent from a simple thought experiment. Consider a generally smooth bed with a number of protrusions, giving a positively-skewed distribution of  $z$ . Now flip the bed upside down to make a generally smooth bed with a number of pits and a negatively-skewed distribution of  $z$ . The standard deviation remains the same, but flow resistance is clearly lower because of the reduction in the frontal area facing the main flow of the river. In principle, therefore, the standard deviation by itself cannot be a perfect predictor of flow resistance.

Recognition of the influence of skewness raises an obvious question: what is the range of skewness in natural river beds? We are not aware of any published information on this. Our analysis (Houseago et al., 2024) of linearly detrended DEMs reveals a difference between coarse alluvial reaches, which all have positive skewness, and bedrock reaches which mostly have negative skewness (Figure 3).

Research taking account of skewness in contexts other than rivers is considered in the next section, but before moving on it is worth noting how river-bed  $\sigma_z$  compares with  $D_{84}$ . The limit case is a uniform bed of tightly-packed spheres. Smart, Duncan, & Walsh (2002) stated that  $\sigma_z/D = 0.17$  for a rectangular array of hemispheres, and Pearson et al. (2017) found a similar ratio in their investigation of ways to estimate grain size from DEMs. With natural poorly-sorted channel beds, one might expect the  $\sigma_z$  values for different sites to be linearly correlated with  $D_{84}$  but with substantial scatter because of differences in grain shape and arrangement. Figure 3c in Aberle and Smart (2003), Figure 4 in Aberle and Nikora (2006) and Figure 4 in Zimmerman (2010) all show such a pattern for flume experiments

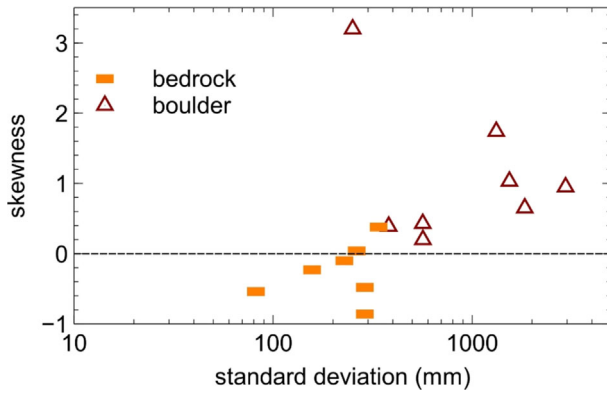


**FIGURE 3** Skewness and standard deviation of vertical deviations from linearly detrended DEMs of alluvial and semi-alluvial reaches. The “boulder” reaches have at least 10% boulder cover and no more than 7% exposed bedrock. The “bedrock” sites have up to 22% sediment cover but no boulders.

using poorly sorted gravel, with  $\sigma_z/D_{84}$  about 0.4 on average. Data from field investigations show more scatter. Nitsche et al. (2012) found only a weak and nonlinear correlation between  $\sigma_z$  and  $D_{84}$  in steep boulder-bed reaches, and the plot of  $\sigma_z$  against  $D_{84}$  in Chen et al. (2020) shows still more scatter even when reaches containing large woody debris are ignored: the lower limit of  $\sigma_z/D_{84}$  is  $\sim 0.2$  and the upper limit  $\sim 1.4$ .

#### 4 | USE OF ROUGHNESS STATISTICS TO PREDICT FRICTION ON MANUFACTURED SURFACES

Rough-bed rivers are unlike most other turbulent boundary layers in having a free surface fairly close to the rough boundary. In the atmospheric boundary layer, and in many engineering contexts, there is instead a free-stream velocity high above the surface with a logarithmic velocity profile for most of the intervening height range. There is extensive literature in boundary-layer meteorology and various branches of engineering offering ways to predict log-law  $k_s$  from surface metrics. In many engineering contexts the root-mean-square roughness, our  $\sigma_z$ , is used as the starting point. At this point, we restrict attention to research that has tried to improve predictions of  $k_s$  by taking account of skewness as well as  $\sigma_z$ , motivated by the peaks versus pits thought experiment. In marine engineering, for example, biofouling (e.g. barnacle growth) on the hull of a ship is recognised to have much more influence on drag and fuel efficiency than pitting of the metal by corrosion or impacts (Sarakinis & Busse, 2022).

The first thorough attempt to establish a predictive relation for  $k_s$  as a function of both  $\sigma_z$  and  $\gamma$  was by researchers from the US Naval Academy (Flack & Schultz, 2010). They obtained data from previous laboratory measurements of pressure drops and velocity profiles in turbulent water flow through ducts with rough surfaces. The surfaces had skewness in the range  $-0.46$  to  $1.51$  and included sandpaper, gravel, packed spheres and arrays of pyramids. The  $k_s$  values determined from velocity-profile measurements were well predicted by the nonlinear relation

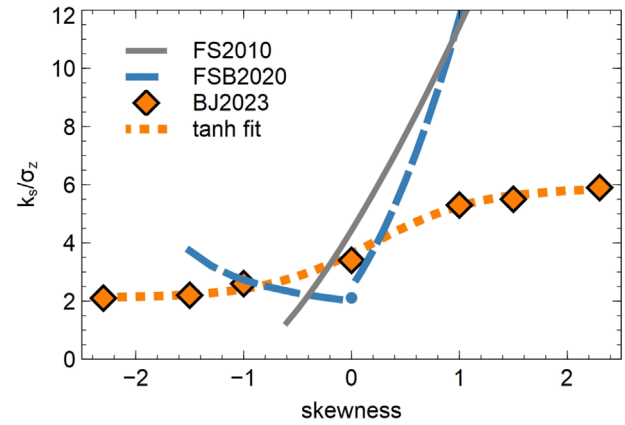


**FIGURE 4** Relation of equivalent sand roughness to surface standard deviation and skewness in duct experiments (Flack & Schultz, 2010; Flack, Schultz, & Barros, 2020) and numerical simulations (data points from Busse & Jelly, 2023; curve is our Equation 8). Curves are truncated at the limits of the skewness ranges to which they were fitted.

$$k_s/\sigma_z = 4.43(1 + \gamma)^{1.37} \quad (6)$$

in which  $\sigma_z$  acts as a scale factor accounting for differences in roughness amplitude. This relation predicts a big increase in  $k_s/\sigma_z$  (from  $<2$  to  $>15$ ) over the range of skewness to which it was fitted. In a later analysis of some of the same data together with new experimental results for random roughness, Flack, Schultz, & Barros (2020) proposed separate correlations for positive, zero and negative skewness:

$$k_s/\sigma_z = 2.48(1 + \gamma)^{2.24} \quad (\gamma > 0) \quad (7a)$$

$$k_s/\sigma_z = 2.11 \quad (\gamma = 0) \quad (7b)$$

$$k_s/\sigma_z = 2.73(2 + \gamma)^{-0.45} \quad (\gamma < 0) \quad (7c)$$

The first of these again predicts very high  $k_s$  values at high positive skewness (Figure 4).

Engineering researchers are increasingly using large-eddy simulation (LES) or direct numerical solution (DNS) of the Navier–Stokes equations to investigate turbulent flow over surfaces with different roughness statistics. The domain for these computational models is almost always a duct with identical rough upper and lower boundaries, between which velocity reaches a maximum at mid-height. The ratio of duct half-height to roughness amplitude is typically of order 10. This vertically-symmetric configuration is computationally simpler than simulating a free-surface flow or a boundary layer of indefinite height. The pressure-drop gradient along the domain enables the overall friction factor to be calculated, and the values of  $y_0$  and  $k_s$  can be estimated from a semi-log plot of the space- and time-averaged fluid velocity at different heights in the lower half of the domain.

A relevant recent example is the work of Busse and Jelly (2023), who used DNS to model flow along a duct with stochastically-generated rough boundaries. Four surfaces were generated with the same roughness amplitude (which constrains  $\sigma_z$  to be near-constant) but different skewness in the range  $0$ – $2.3$ , and the three

positively-skewed surfaces were flipped to create three negatively-skewed surfaces. The seven simulations indicated a very different pattern of variation in  $k_s/\sigma_z$  with  $\gamma$  than had been suggested by either Flack and Schultz (2010) or Flack, Schultz, and Barros (2020):  $k_s/\sigma_z$  was found to approach constant values at large negative or large positive skewness, being higher in the latter case. Busse and Jelly (2023) proposed a hyperbolic tangent function of  $\gamma$  as a predictor of the upward shift in the fitted log-law profile. They did not give an expression for  $k_s$ , but we find that the values of  $k_s/\sigma_z$  plotted in Figure 5b are fitted well by

$$k_s/\sigma_z = 1.9 \tanh(\gamma - 0.2) + 4.0 \quad (8)$$

The data points and our fit to them are shown in Figure 4.

Each of these three papers finds lower resistance for negatively-skewed ('pits') than positively-skewed ('peaks') roughness, as expected, but the lack of quantitative agreement between the laboratory and computational results strongly suggests that skewness is not a sufficient predictor. By implication, other aspects of surface topography are also relevant and they must have differed between the surfaces considered by the different authors.

## 5 | ARRAYS OF LARGE ROUGHNESS ELEMENTS

In many non-fluvial contexts, it is natural to think in terms of a plane bed on which is superimposed an array of individual roughness elements. Much research on atmospheric boundary layers has been concerned with built environments in which more-or-less cuboid buildings protrude above a more-or-less flat ground surface. Another important strand focuses on the effects of vegetation canopies on air flow near the ground, and there is a small literature on how stones or patchy vegetation inhibit soil erosion by wind or overland flow. There is also a large and rapidly growing engineering literature concerned with how irregularities on smooth manufactured surfaces affect turbulence and drag; this includes research on aeronautics, the flow of gases within machinery and ship movement through seawater.

Some river beds can also be thought of in this way. Many steep coarse-bed channels contain boulders protruding above relatively finer (though usually still coarse) sediment. Treating the boulders differently from the rest of the bed can involve an arbitrary cutoff if the grain-size distribution is unimodal with no obvious inflection, but in some channels there are essentially two different scales of roughness and the grain-size distribution is inflected or even bimodal. This is often due to the presence of immobile boulders, distinctly larger than the rest of the bed, that have fallen into the channel from steep valley walls (Shobe, Tucker, & Anderson, 2016) or been exhumed from

glacial deposits (Polvi, 2021). It also occurs where boulders and large cobbles form relatively immobile channel-spanning steps (Yager, Dietrich, 2012). In bedrock channels that follow the dip of sedimentary strata, joint blocks can be plucked from steps or fall from sidewalls to create boulder arrays on a relatively smooth bed (Ferguson et al., 2017); conversely, if the strata are tilted the bedrock itself can have protruding ribs or towers (e.g. Goode & Wohl, 2010). Four of these situations are illustrated in Figure 1. The characteristics of a boulder array are typically measured manually, but if a high-resolution DEM is available it may be possible to identify large bed elements from the difference between the detailed DEM and a smoothed version of it (Wiener & Pasternak, 2022).

### 5.1 | Drag on obstacles

If a boundary can reasonably be conceptualised as an array of large roughness elements protruding above a smoother bed, the flow resistance imparted by the large elements can be calculated from standard physical principles. The drag force  $F_D$  exerted by an object protruding into a fluid is

$$F_D = \rho A_f u^2 C_D / 2 \quad (9)$$

where  $\rho$  denotes fluid density,  $A_f$  is the flow-facing (frontal, cross-sectional) area of the object,  $C_D$  is its drag coefficient and  $u$  is the average fluid velocity approaching the object. If many such objects exist within a total planar bed area  $A$ , and the low parts of the bed make a negligible contribution to total flow resistance, the total drag force now involves  $\Sigma A_f$  and can be equated with the product of  $A$  and the mean shear stress  $\tau$ . This yields

$$\tau = \rho (\Sigma A_f / A) u^2 C_D / 2 \quad (10)$$

Extra terms can be added for skin friction on obstacle tops and the bed between obstacles; if so, the shear stress on each roughness component is its drag force divided by its planar bed area. The ratio  $\Sigma A_f / A$  is usually denoted by  $\lambda_f$  and is variously referred to as the frontal area ratio, frontal density or frontal solidity. The drag coefficient depends on the shape of the object, the spacing between multiple objects, and whether obstacles are fully, or only partly, submerged; it also depends on the flow Reynolds number if the flow is only transitionally rough, as can be the case in some engineering contexts.

The large-scale structure of flow over a large-element array varies with the frontal solidity of roughness elements, and thus to some extent also with their spatial density (the ratio  $\lambda_p$  of their total plan area to the reach area  $A$ ). If the elements are identical and have the same vertical and horizontal dimensions,  $\lambda_f$  increases in direct proportion to  $\lambda_p$ . Three qualitatively different regimes occur as  $\lambda_f$  and  $\lambda_p$

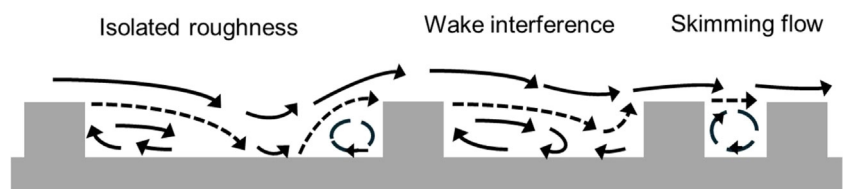


**FIGURE 5** Schematic diagram of how the spacing of roughness elements affects the near-bed flow structure. Flow separation occurs below the dashed stream lines.

increase: 'isolated roughness', 'wake interference' and 'skimming flow' (Morris, 1955). As sketched in Figure 5, at very low values of  $\lambda_p$  and  $\lambda_f$  the wake from each obstacle does not extend as far as any other obstacle, so the total drag increases with  $\lambda_p$ . Eventually, some wakes do extend to other obstacles which therefore have a reduced effective frontal area (or a reduced approach velocity if averaged over the entire frontal area) and an altered drag coefficient because of the change in the pressure field around the downstream obstacle (e.g. Nepf, 1999). As  $\lambda_p$  and  $\lambda_f$  increase within this wake-interference regime, there are more obstacles but less drag per obstacle. Resistance to flow reaches a maximum within this regime, typically at a frontal solidity of around 0.2 although the precise value depends on obstacle shape and arrangement. Eventually, the entire base plane is within wakes and the main flow is skimming the roughness tops, with less overall drag. Similarly, the height at which turbulence intensity is greatest increases progressively with  $\lambda_p$  (e.g. Nowell & Church, 1979). In the limit,  $\lambda_p = 0$  and 1 both correspond to a completely uniform bed with lower flow resistance than at any intermediate element density.

## 5.2 | Free-surface flow over obstacles

Equations (9) and (10) apply to any turbulent boundary layer. In the specific case of a flume or river, the flow is fully rough and as Bathurst (1978) pointed out, we also know that for steady uniform flow  $\tau = \rho gRS = \rho v^2 f/8$  where  $v$  as before is the overall mean velocity. This leads to

$$(8/f)^{1/2} = 1/\left[\lambda_f(u/v)^2 C_D/2\right]^{1/2} \quad (11)$$

for the total flow resistance if the rest of the bed makes a negligible contribution; an extra term can be added if necessary. This equation is of little or no practical value but it shows the two-way interaction between local and overall scales. Locally, the drag on an individual boulder depends on the approach-flow velocity  $u$ , the upper limit of which is the overall mean velocity  $v$ ; but  $v$  depends on the spatial density and arrangement of the boulders. At a given discharge  $v$  decreases from low to moderate obstacle density, then increases again. The approach velocity averaged over the full frontal area of a representative obstacle decreases towards zero as  $\lambda_p$  and  $\lambda_f$  increase and wakes become wider and deeper. The approach velocity may also vary across the channel (e.g. lower near the banks); this led Judd and Peterson (1969) and Bathurst (1978) to argue that the overall flow resistance ought to vary with the channel's width-depth ratio as well as with relative submergence.

The interdependence of  $u$  and  $v$  is not the only difficulty facing any practical use of Equation (11): it is also necessary to assign a value to the drag coefficient. Textbooks generally give  $C_D \sim 1$  for turbulent flow past a cube,  $\sim 1.2$  for a cylinder and  $\sim 0.4$  for a hemisphere, so a well-submerged boulder probably has a drag coefficient between these limits. Schmeekle, Nelson, and Shreve (2007) and Lamb and Brun (2017) measured values of  $\sim 0.9$  and  $\sim 0.7$ , respectively, for natural pebbles submerged in a flume. However, flume investigations of flow over an isolated hemisphere have shown that the drag coefficient decreases with increasing submergence, and when the water

surface is close to or below the top of the obstacle the drag coefficient can be much higher ( $\sim 2$  or more) because of wave drag (Flammer, Tullis, & Mason, 1970; Lamb & Brun, 2017). Computer simulations of free-surface flow round and over isolated boulders are consistent with these experimental findings and give details of the turbulent structures involved (Thappeta et al., 2017).

The drag coefficient for obstacles in most rivers will differ from that for simple cylinders or spheres because of the effects mentioned above and other factors. For example, Yager, Dietrich (2012) found that the boulder drag coefficient in step-pool streams needed to be much higher than that for a sphere, cylinder or cube to correctly predict the measured flow velocity. In such cases, significant resistance occurs from plunging flow over the steps, and surface waves and hydraulic jumps that are not captured in a simple drag equation. The drag coefficient in Equation (9) indirectly translates simple areas and velocities into drag forces that are controlled by the complex pressure field around an obstacle. In many field applications,  $C_D$  is not really a drag coefficient for pressure drag around individual obstacles, but more of a bulk resistance coefficient like  $f$ . In such cases,  $u$  is often assumed to be effectively equal to the mean flow velocity and Equation (11) is replaced with stress-partitioning equations that account for different roughness sources (e.g. Manga & Kirchner, 2000; Yager, Dietrich, 2012; Yager, Turowski, 2012; Yager, Kirchner, & Dietrich, 2007).

Notwithstanding these problems, boulder-drag calculations have been used to show that immobile boulders in mountain rivers have important consequences: by extracting momentum from the flow, they inhibit bedload transport (Yager, Dietrich, 2012; Yager, Turowski, 2012; Yager, Kirchner, & Dietrich, 2007) and bedrock incision (Shobe, Tucker, & Anderson, 2016). The extent of the calculated effect is obviously dependent on the assumed drag coefficient.

Several researchers have estimated flow resistance from measurements in flumes, or in one case rivers (Bathurst, 1978), and related it to array metrics and/or relative submergence. Herbich and Shulits (1964) reported results from flume experiments with partly- and fully-submerged cubic blocks in different arrangements. Their Figure 16 showed that Manning's  $n$  (and therefore also  $f$ ) increased from low to intermediate ( $\sim 0.25$ ) values of a density index similar to  $\lambda_f$ , and did not differ greatly between random and regular arrangements. The field investigation by Bathurst (1978) was unusual in that he defined as boulders only those clasts that protruded above the water surface so that at higher discharge there were fewer of them and his measured values of  $\lambda_p$  and  $\lambda_f$  decreased. He attempted to correlate  $\lambda_p$  and  $\lambda_f$  with  $D_{84}/R$  and thus establish a relative-submergence resistance equation. Nitsche et al. (2012) found that errors in relative-submergence predictions of velocity in steep boulder-bed streams were correlated with boulder concentration. Yager, Kirchner, and Dietrich (2007) used flume experiments to test a stress-partitioning theory and found that the effects of simulated boulder spacing and boulder protrusion (height above the surrounding bed) exerted strong controls on predicted flow conditions, with the highest measured resistance at intermediate boulder spacings. Their results also demonstrated that  $\lambda_f$  can vary at a fixed  $\lambda_p$ : boulders can become partly buried by finer sediment, which reduces their protrusion and therefore  $A_f$  and  $\lambda_f$ . For the same  $\lambda_p$ , greater boulder protrusion results in higher predicted drag and lower estimated velocities. Changes in boulder protrusion can result from temporal fluctuations in the upstream sediment supply. Bedload transport predictions that incorporated

variation in protrusion, and therefore  $\lambda_f$ , performed better in both flume experiments and a step-pool stream (Yager, Turowski, 2012; Yager, Kirchner, & Dietrich, 2007).

Some flume experiments by Italian researchers have used natural pebbles or quarry rubble to create obstacle arrays on a bed of fine gravel. Ferro and Giordano (1991) found that flow resistance increased with the spatial density of the coarse clasts, but  $D_{84}$  also increased so that  $h/D_{84}$  remained a fairly good predictor in a logarithmic resistance equation. Baiamonte and Ferro (1997) subsequently showed that the log-law  $k_s$  value reached a maximum at  $\lambda_p \sim 0.15$ . Canovaro, Paris and Solari (2007) compared transverse stripe, random and longitudinal stripe arrangements of the coarse clasts and found that flow resistance decreased in that order for a given spatial density, and was highest at densities of 0.2 to 0.4.

At a smaller scale, overland flow can be retarded by stones protruding above the soil surface. Lawrence (1997) used obstacle-drag and mixing-length arguments to propose different velocity profiles for overland flow past partially- and fully-immersed hemispheres of height  $k$ . Her partial-immersion model assumed a fixed drag coefficient and had the counter-intuitive implication that  $(8/f)^{1/2}$  would decrease with increasing depth (i.e. resistance would increase). The fully-immersed model gave a simple proportionality between  $(8/f)^{1/2}$  and the relative submergence  $d/k$ . This linear relation has also been found to give an excellent fit to gravel-bed flume measurements (Aberle & Smart, 2003; Rickenmann, 1991), and forms the shallow-flow asymptote of the variable-power resistance equation (Ferguson, 2007). Lawrence (2000) reported flume experiments designed to test her earlier proposals. She found much greater resistance than predicted in the partially-immersed regime, implying that the assumption of constant  $C_D$  was wrong, and attributed this to wave drag around obstacle tops. For well-inundated obstacles, the effective roughness height was similar to the root-mean-square elevation of the hemispheres rather than their maximum height.

### 5.3 | Atmospheric flow over roughness element arrays

Theory for flow over obstacles has been developed most fully in boundary-layer meteorology. Some of it relates to dense tree canopies and is more relevant to flow in lowland rivers with stiff vegetation than to rough-bed rivers, but a sparse tree canopy is not dissimilar to an array of quasi-cylindrical boulders protruding from a shallow stream. Other strands of the meteorological literature are about wind flow over buildings or sparsely-vegetated soil. These contexts are more comparable to river flow over submerged boulders, though with the important difference that there is no free surface: instead, the upper limit of the boundary layer is the mean free-stream wind speed high above the ground surface. One consequence of this difference is that textbook values for the drag coefficients of solid obstacles are much more reliable in the atmospheric boundary layer than in shallow open channels where free-surface effects are important.

Almost all research on atmospheric boundary layers starts from the assumption of a logarithmic velocity profile that starts a little way above the roughness tops and is subject to a zero-plane displacement  $d$ , with  $y/y_0$  replaced by  $(y-d)/y_0$  in Equation (1). The research aim has

usually been to determine the partitioning of shear stress between obstacles and intervening ground, and the dependence of  $y_0$  (and thus  $k_s$ ) on the spatial density  $\lambda_p$  and/or frontal solidity  $\lambda_f$  of obstacles. These problems have been investigated partly by wind-tunnel experiments and partly from theoretical considerations. In the latter case, a subsidiary problem is how the ratio of displacement height  $d$  to obstacle height  $k$  varies with obstacle density.

Wind-tunnel measurements of flow resistance over obstacle arrays (e.g. Raupach, Thom, & Edwards, 1980) show similar results to flume experiments: resistance increases to a broad maximum at a frontal solidity of  $\sim 0.2$  and then declines. The first quantitative model that extended from the isolated-roughness regime into the wake-interference regime was proposed by Raupach (1992). This influential paper used scaling arguments for how the volume and bed area of a wake vary with obstacle height ( $k$ ) and width and thus quantified how the volume and bed area of the sheltered part of the flow increase with obstacle density. Depending on the precise values assumed for the bed and obstacle drag coefficients,  $k_s/k$  is predicted to increase to a near-constant value of  $\sim 3$  at a frontal solidity of  $\sim 0.5$ , which is the limit of applicability of the model. The proportion of total friction that is generated by obstacles exceeds 90% for  $\lambda_f > 0.1$ . Raupach (1992) showed that the model was consistent with experimental results from wind tunnels at low to moderate frontal densities.

Models that include the transition to skimming flow were subsequently developed by Macdonald, Griffiths, and Hall (1998) and Shao and Yang (2005, 2008). Both groups of researchers assumed that the velocity profile is logarithmic with a displacement height that increases from 0 to  $k$  as  $\lambda_p$  increases from 0 to 1. The three papers differ in whether they model this increase in  $d$  or the associated reduction in effective frontal area, exactly how they do it, and whether or not they allow for skin drag on obstacle tops. The model of Macdonald, Griffiths, and Hall (1998) for obstacles of height  $k$  predicts  $y_0$  as

$$y_0/k = (1 - d/k) \exp\left\{-[0.5\beta C_D(1 - d/k)\lambda_f/k^2]^{1/2}\right\} \quad (12a)$$

with the displacement height  $d$  given by

$$d/k = 1 - A^{-\lambda_p} (\lambda_p - 1) \quad (12b)$$

The coefficient  $\beta$  has an empirical value of 0.55 for cubes and the coefficient  $A$  has a best-fit value of 4.43 for a staggered array of cubes or 3.59 for a square array. Illustrative results from this model later in our review are calculated using  $A = 4$ .

The Macdonald et al. model and the two proposed by Shao and Yang (2005, 2008) all successfully reproduce the qualitative behaviour observed in wind-tunnel and flume experiments with arrays of sharp-edged obstacles: log-law  $k_s$  increases to a maximum at  $\lambda_p \sim 0.2$  and then declines at higher obstacle densities. For uniform cubes, each model predicts a peak value of  $k_s/k$  of about 3 to 4 depending on the assumed drag coefficient. For non-cubic roughness elements, the peak value of  $k_s/k$  varies substantially according to frontal solidity and drag coefficient but occurs at roughly the same spatial density. Figure 6 illustrates this for cubes and hemispheres of height  $k$ , and cuboids of height  $k$  and plan dimensions  $2k$  by  $k$  that are either aligned with the flow (so lower frontal area) or transverse to it. The curves for cubes and transverse cuboids are identical since at a given spatial density

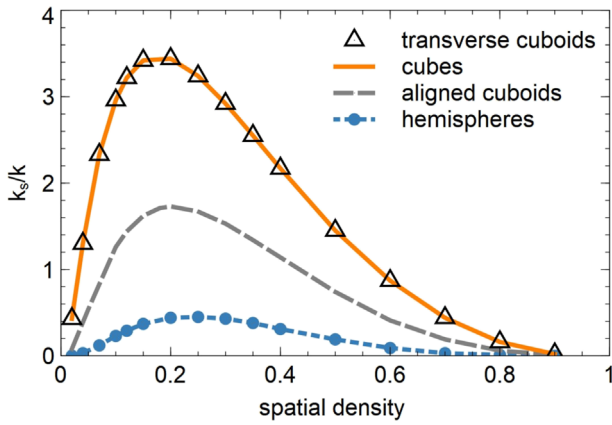


**FIGURE 6** Equivalent sand roughness  $k_s$ , normalised by obstacle height  $k$ , for different types of uniform roughness element according to the model of Macdonald, Griffiths, & Hall (1998). Drag coefficient taken as 1.0 for cubes and cuboids, 0.4 for hemispheres.

there are twice as many cubes as transverse cuboids but each cube has only half the frontal area of a transverse cuboid.

All these models assume an array of identical obstacles and take no account of their spatial arrangement. Buildings in urban areas are of course far from identical in height and shape, as emphasised by Grimmond and Oke (1999) who showed that field or laboratory-model estimates of  $\gamma_0$  and  $d$  for parts of cities do not show any clear relation to  $\lambda_p$  or  $\lambda_f$ . The effect of heterogeneity in height has been investigated using LES simulations (Xie, Coceal, & Castro, 2008) and theoretically (Millward-Hopkins et al., 2011). Xie, Coceal, and Castro (2008) simulated air flow over a regular array of buildings with  $\lambda_p = 0.25$  and normally-distributed heights. They found that the tallest buildings generated disproportionate contributions to total drag and turbulent kinetic energy. Millward-Hopkins et al. (2011) developed a model similar to that of Raupach (1992) but allowing for a distribution of obstacle height and some sheltering alongside obstacles as well as in their lee. The taller obstacles experience little or no sheltering but have extensive wakes that may completely shelter any adjacent low obstacles so that the effective frontal solidity is reduced and the effective mean obstacle height is increased. The wakes from isolated tall obstacles survive even when there is skimming flow over the lower obstacles, so full skimming flow cannot develop and the curve of  $k_s/k$  against  $\lambda_p$  (where  $k$  is now an average obstacle height) reaches a plateau rather than a maximum followed by a decline. The ratios  $k_s/k$  and  $d/k$  were found to depend as much or more on the variance of obstacle height as on obstacle density. Although these papers were motivated by problems involving air flow over and round buildings, they appear relevant to the water flow over heterogeneous boulder arrays.

An obstacle-array model that takes account of spatial arrangement as well as mixed-height obstacles was proposed by Yang et al. (2016). It assumes an exponential velocity profile within the roughness layer, merging into a logarithmic profile higher up and an eventual free-stream velocity. The key novelty is an iterative calculation of how much of the total fluid volume in the roughness layer is sheltered by upstream obstacles. If the obstacles differ in height, with mean  $k_m$  and standard deviation  $s_k$ , the top of the roughness layer is taken to be at  $k_m + s_k$ .

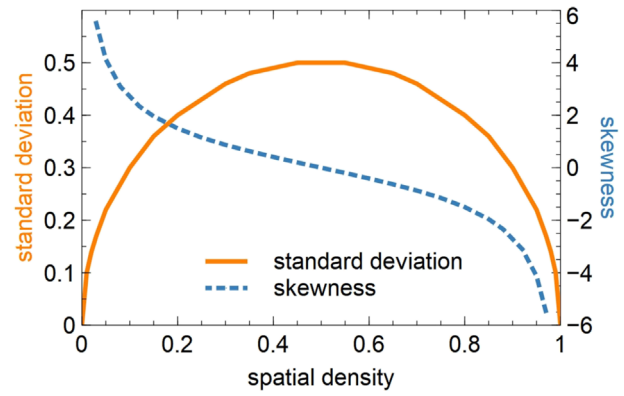


**FIGURE 7** Moment statistics of unit-cube ( $k = 1$ ) arrays of different spatial density.

## 6 | LINKS BETWEEN ROUGHNESS STATISTICS AND ARRAY-RELATED METRICS

Thus far we have discussed moment statistics and obstacle arrays as distinct approaches to flow resistance, but it is possible to combine elements of both approaches. In this section, we show that statistical moments can be calculated for obstacle arrays and that particular obstacle metrics form pairs with particular roughness statistics that have broadly equivalent effects on flow resistance.

The obstacle arrays considered by the boundary-layer meteorology community seem highly idealised in comparison to the irregularity of most river beds, and the instinct of many fluvial geomorphologists will be to prefer statistical metrics of roughness. But if statistical metrics are to be effective predictors of flow resistance, it is reasonable to expect that they work for regular obstacle arrays as well as for quasi-random surfaces. Conversely, it is interesting to see what the obstacle-array models imply about the variation of drag with skewness.

### 6.1 | Moment statistics of arrays

It is mathematically straightforward to obtain the first few moment statistics of arrays of cuboid roughness elements. This provides some further insight into both the value of  $\sigma_z$  as a roughness metric and its limitations. For an array of cubes of height  $k$ , the standard deviation is

$$\sigma_z = k[\lambda_p(1-\lambda_p)]^{1/2} \quad (13)$$

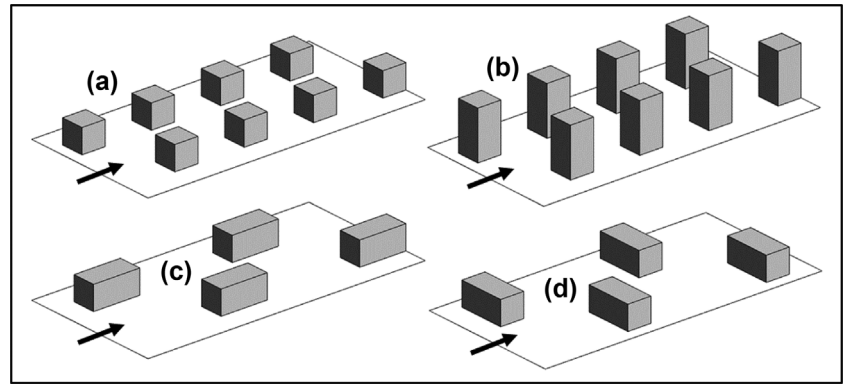
which rises and falls symmetrically as  $\lambda_p$  increases from 0 to 1 (Figure 7), and is proportional to  $k$  as expected on scaling grounds. The skewness is

$$\gamma = (1-2\lambda_p)/[\lambda_p(1-\lambda_p)]^{1/2} \quad (14)$$

which is independent of  $k$ , as befits a nondimensional statistic. It has decreasing positive values as  $\lambda_p$  increases from 0 to 0.5, then gradually larger negative values in the skimming-flow regime (Figure 7).

Comparison of Figure 7 with Figure 6 demonstrates again the limitations of  $\sigma_z$  on its own as a predictor of flow resistance, and the

**FIGURE 8** Four possible arrangements of cube or cuboid obstacles, all with the same spatial density  $\lambda_p = 0.111$ : (a) cubes, (b) upright cuboids, (c) aligned cuboids, (d) transverse cuboids. Flow from left, frontal areas shaded black.



desirability of taking skewness into account. For any two cube arrays with the same  $\sigma_z$  (e.g.  $\lambda_p = 0.1$  and  $0.9$ , or  $0.2$  and  $0.8$ ), obstacle drag is greater in the isolated-roughness regime (plane bed with sparse obstacles,  $\lambda_p$  low,  $\gamma > 0$ ) than in the skimming-flow regime (plane bed with sparse pits,  $\lambda_p$  high,  $\gamma < 0$ ). This suggests that the skewness of a quasi-random surface may play a broadly equivalent role to the spatial density of an obstacle array. Low density is associated with positive skewness and relatively high drag, and high density with negative skewness and relatively low drag.

## 6.2 | Comparing engineering correlations and obstacle-array models

We have seen that  $\sigma_z$  by itself cannot be a perfect predictor of flow resistance, whereas engineering-literature relations like Equations (6), (7) and (8) above that use both  $\sigma_z$  and  $\gamma$  can in principle get closer to capturing the variation of flow resistance with the spatial density of obstacles. But when those equations are applied to obstacle arrays, it emerges that they cannot be perfect predictors either. This can be seen by considering different possible arrays of cuboid obstacles measuring  $2k$  by  $k$  by  $k$  (Figure 8). The skewness as given by Equation (14) remains the same for cuboids as for cubes, irrespective of the orientation of the cuboids, because the greater height of upright elements is offset by their smaller footprint. The standard deviation as given by Equation (13) depends on obstacle orientation. Compared to the value for cubes,  $\sigma_z$  is doubled for upright cuboids, so Equations (6–8) correctly predict higher sand-equivalent roughness. But if the long axis of each cuboid is horizontal,  $\sigma_z$  and  $\gamma$  are the same as for cubes irrespective of the orientation of the cuboids. Any correlation using only  $\sigma_z$  and  $\gamma$  then predicts the same value of  $k_s$  whether the long axis is transverse to the flow (maximising drag) or aligned with it (minimising drag), because it does not capture the difference in frontal area.

The meteorological models for obstacle arrays do involve  $\lambda_f$ , and predict less drag and lower  $k_s$  for aligned cuboids than for the other configurations with the same spatial density. By making use of the relations of  $\sigma_z$  and skewness to obstacle density (Equations 13 and 14) it is possible to plot predictions of  $k_s/\sigma_z$  by the Macdonald, Griffiths, & Hall (1998) model against skewness, thus allowing comparison with the engineering correlations illustrated in Figure 3. We do this in Figure 9 for the four array types in Figure 8, but now varying the spatial density of obstacles.

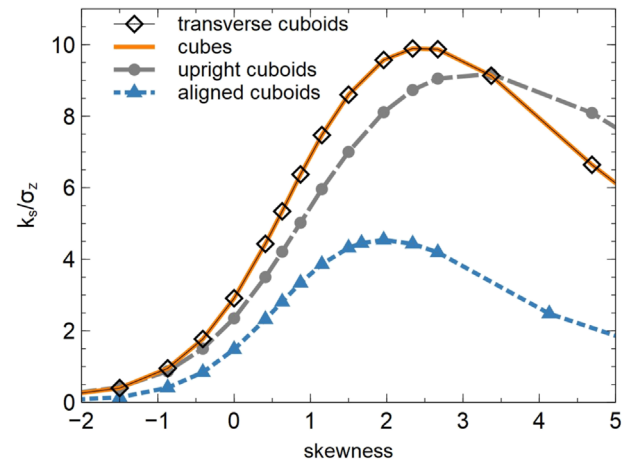


**FIGURE 9** Effective sand roughness  $k_s$ , normalised by  $\sigma_z$ , as predicted by the model of Macdonald, Griffiths, and Hall (1998) for cube or cuboid arrays with  $C_D = 1.0$ . Plotted points correspond to different values of spatial density  $\lambda_p$  (progressively higher from right to left along each curve) and consequently different skewness and standard deviation.

Comparison of Figure 9 with Figure 4 shows major differences. The engineering correlations of Equations (6) and (7) (Flack & Schultz, 2010; Flack, Schultz, & Barros, 2020), based as they are on experimental results for a narrow range of skewness, predict very high resistance (as quantified by  $k_s/\sigma_z$ ) when extrapolated to block arrays that are sparse (high positive skewness) or dense (high negative skewness). In contrast, the aerodynamic models for obstacle arrays predict very low resistance at high negative skewness, and less resistance at the highest positive skewness values than at more moderate ones. The DNS results of Busse and Jelly (2023) that are plotted in Figure 4, and our tanh fit to those results (Equation 8), are more consistent with the obstacle-array literature insofar as the DNS results indicate least resistance at high negative skewness. Equation (8) and the data to which we fitted it show a plateau in resistance at higher positive values of skewness. This is unlike the peak then decline shown in Figure 8 for arrays of homogeneous obstacles, but is not dissimilar to what Millward-Hopkins et al. (2011) predicted for arrays of mixed-height obstacles. These discrepancies between the implications of theoretical models, engineering correlations and numerical simulations suggest there is still some way to go in reconciling the moment-statistics and obstacle-array approaches.

### 6.3 | Effective slope

Several other roughness metrics have been suggested in the engineering literature. One section of a wide-ranging review by Chung et al. (2021) is devoted to all the possibilities. Many of them are more appropriate for obstacle arrays on a plane than for irregular surfaces, but one that integrates the two perspectives is the effective slope (ES) index that was introduced by Napoli, Armenio, and De Marchis (2008). ES is defined as the mean of the absolute value of  $\partial z/\partial x$  along an x-direction line:

$$ES = \frac{1}{L} \int_0^L \left| \frac{\partial z}{\partial x} \right| dx \quad (15)$$

where L is the length of the line. The equivalent finite-difference definition of ES for the centre-line longitudinal profile of a river bed is  $ES = \langle |\Delta z/\Delta x| \rangle$ , and an overall ES value for a gridded DEM can be calculated similarly. Vertical stretching of a rough surface increases ES and  $\sigma_z$  to the same extent, but surfaces with the same standard deviation can differ in effective slope depending on roughness geometry. ES was stated by Napoli, Armenio, and De Marchis (2008) to be mathematically equivalent to  $2\lambda_f$  for an obstacle array, so has the potential to play the same role in resistance calculations for irregular surfaces as  $\lambda_f$  does for obstacle arrays.

Napoli, Armenio, and De Marchis (2008) ran quasi-DNS simulations of flow over surfaces with superimposed corrugations of random amplitude and found that as ES increased from 0.05 to 0.8 the pressure drag component of total shear stress increased rapidly then more slowly, becoming almost constant at  $ES > 0.5$ . The friction drag component showed the opposite pattern, dominating at low values of ES but becoming smaller than the pressure component at  $ES > 0.15$  and negligible at  $ES > 0.5$ . These authors did not present values of  $k_s$  or  $\sigma_z$ , but as discussed below a later DNS-based paper by Forooghi et al. (2017) includes a plot of  $k_s/\sigma_z$  against ES that shows an initially rapid, then progressively slower, increase with ES. Our own analyses of rough-bed river DEMs suggest that ES values range very widely: 0.13 to 0.94 with a median of 0.36. The lowest values are for smooth bedrock and the highest for reaches with high boulder density so that ES is positively correlated with  $\sigma_z$  in this particular sample of sites.

The ES index also features in the part of Chung et al.'s (2021) review paper that discusses what minimal subset of roughness metrics needs to be included in a widely-applicable predictive relation for flow resistance. They suggest that the answer is likely to be

$$k_s/k = \text{function}(\lambda_f \text{ or } ES, \lambda_p \text{ or skewness}) \quad (16)$$

where k is some metric of roughness amplitude. This suggestion of a minimal set is consistent with our findings earlier in the present paper: we have shown that neither  $\sigma_z$  on its own (acting as k in Equation 16), nor  $\sigma_z$  in combination with  $\gamma$ , can discriminate between idealised situations that are intuitively likely to have different resistance to the same flow. The ES index appears to be a promising addition to these two moment statistics.

Forooghi et al. (2017) investigated the separate effects of skewness and effective slope on velocity profiles, and thus  $k_s$ , in DNS simulations of deep ( $h/\sigma_z \sim 20$ ) open-channel flow over randomly-arranged arrays of conical or semi-ellipsoid obstacles varying

randomly in height. The surfaces were computer-generated to have the same average roughness amplitude. The authors concluded that a practical correlation could take the form

$$k_s/k = F(\text{skewness}) \bullet G(ES) \quad (17a)$$

and suggested best-fit component functions

$$F = 1.3 + 0.93\gamma + 0.67\gamma^2 \quad (17b)$$

$$G = 1.07(1 - e^{-3.5ES}) \quad (17c)$$

These functions are plotted in Figure 10. They are empirical fits to four values of skewness in a fairly narrow range ( $-0.35$  to  $0.66$ ) and five values of ES in a fairly wide range ( $0.20$  to  $0.88$ ); we show the values used as well as the extrapolated shapes of the fitted functions. The skewness function predicts higher resistance from positively- than negatively-skewed surfaces, as expected. Its quadratic form means that it predicts increased resistance when extrapolated to higher negative skewness, but as Forooghi et al. (2017) noted the behaviour of Equation (17b) beyond the range of the calibration data should be regarded with caution. Comparison with Figure 4 shows that Equation (17b) is not dissimilar to the correlations proposed by Flack and Schultz (2010) and Flack, Schultz, & Barros (2020) but is inconsistent with what Busse & Jelly (2023) found for high positive and negative skewness. The ES function suggests a much greater sensitivity of resistance to ES at lower values, which is consistent with Napoli, Armenio, and De Marchis (2008).

One way to check how well Equation (17) extrapolates to different surfaces is to apply it to arrays of sharp-edged obstacles (cubes or cuboids) rather than the conical or half-ellipsoid ones to which it was calibrated. This can be done by making use of the equivalence of ES with  $2\lambda_f$ . We have already seen that urban meteorology models such as that of Macdonald, Griffiths, and Hall (1998) predict a peak in  $k_s$  at a fairly low obstacle density ( $\lambda_p$  and  $\lambda_f$  around 0.1 to 0.3), with less resistance in the isolated-roughness ( $\lambda_p$  near zero) and skimming-flow ( $\lambda_p$  towards 1) regimes. Figure 11 compares predictions using Equation (17) with those previously displayed in Figure 5 that were generated using the sheltering model of Macdonald, Griffiths, and Hall (1998). The two approaches agree in some respects but not in others. Both predict, as would be expected, that less drag is exerted by cuboids aligned with the flow than by other arrangements. At moderately high spatial densities (0.3 to 0.6) the quantitative predictions are

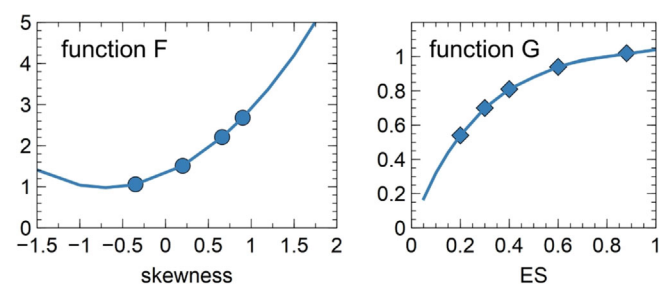


**FIGURE 10** Effects of skewness and effective slope on rough-surface friction as predicted by Equations (17b) and (17c) (Forooghi et al., 2017). Symbols show the data points to which the curves were fitted.

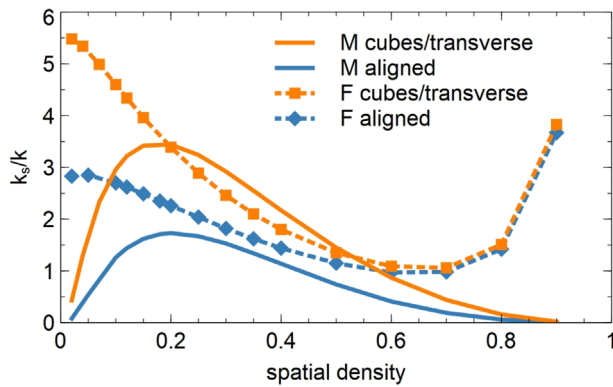


**FIGURE 11** Predicted drag on block arrays: comparison between the sheltering model of Macdonald, Griffiths, and Hall (1998), denoted by M in the legend, and the correlation proposed by Forooghi et al. (2017), denoted by F. Curves in orange are for cubes and transverse cuboids; curves in blue are for cuboids aligned with flow. Sheltering-model predictions assume  $C_D = 1.0$ .

broadly similar, but the Forooghi et al. (2017) correlation does not predict a maximum of drag at any intermediate density:  $k_s/k$  is instead predicted to increase towards the limits  $\lambda_p = 0$  and 1. This is a consequence of the quadratic form which Forooghi et al. (2017) chose when fitting Equation (17b) to a nonlinear, but monotonic, change in  $k_s/k$  over a fairly narrow range of skewness (see Figure 10). The comparison shows again that models and correlations devised for or fitted to particular types of roughness do not necessarily hold when applied to different surfaces.

A similarly pessimistic conclusion about the search for a universal rough wall model was reached in a recent fluids engineering paper (Yang et al., 2023). These authors tested the ability of six models or correlations to extrapolate to new types of surfaces. Four of the candidates have already been discussed: the correlations of Flack and Schultz (2010) using  $\sigma_z$  and  $\gamma$ , the correlation of Forooghi et al. (2017) using  $\sigma_z$  and ES and the obstacle-array models of Macdonald, Griffiths, & Hall (1998) and Yang et al. (2016). The other two are another  $\sigma_z$  and  $\gamma$  correlation (Barros, Schultz, & Flack, 2018), and a machine-learning predictor developed by Jouybari et al. (2021) that was trained on 45 surfaces. Yang et al. (2023) tested how well each model or correlation could reproduce experimental or computational values of  $k_s$  for 68 surfaces. Much of the data used came from the recently-established Roughness Database (n.d.). Some of the candidate models had been calibrated or trained on some of the surfaces, but all were extrapolating to many other surfaces. None of the three statistical correlations performed well, and nor did the machine learning model until it was re-trained on the new data. The Macdonald, Griffiths, & Hall (1998) model predicted too narrow a range of  $k_s$ , mainly through the inability to allow for different arrangements, but the Yang et al. (2016) model with its iterative sheltering calculation did better.

A similar comparative test by Abdelaziz et al. (2024) used measured  $k_s$  values for 120 surfaces, mostly from the Roughness Database but supplemented by the authors' own experiments. The data include open-channel flows as well as other turbulent boundary layers, both regular and irregular roughness, and a near-equal mixture of experimental and numerical results. The correlation proposed by Forooghi et al. (2017), shown in our Equation 17, was the most

successful of six existing predictive relations that were compared; interestingly, it was the only one to include ES as a predictor. Abdelaziz et al. (2024) showed that even better predictions were possible using a relation that includes not only ES but also the product of ES and skewness:

$$k_s/\sigma_z = -7.65 - 0.0013\gamma + 2.90ES + 9.40 \exp(0.705 \gamma ES) \quad (18)$$

The coefficients in this equation were fitted to data, seemingly one predictor at a time as in Forooghi et al. (2017) though this is not entirely clear from the paper. The coefficient values imply that for a given value of  $\sigma_z$ ,  $k_s$  increases with skewness and does so more rapidly when ES is higher.

## 6.4 | Other factors affecting total resistance

Even when three metrics are used to predict  $k_s$ , as in the generic proposal of Equation (16) and the specific proposals of Equations (17) and (18), it is unlikely that perfect predictions can be obtained even for the type of surface to which the correlation has been calibrated. Chung et al. (2021) note that clustering and directionality are important complications that have been demonstrated to affect the total drag of different surfaces with the same roughness amplitude and skewness.

We noted earlier that flume experiments by Canovaro, Paris and Solari (2007) revealed differences in resistance when the same number of miniature 'boulders' were arranged in transverse stripes, longitudinal stripes or randomly. The DNS simulations of Forooghi et al. (2017) showed something similar: a staggered array of obstacles gave more drag than an aligned array, with random placement in between but closer to the staggered arrangement. Fang, Liu, and Stoesser (2017) suggested on the basis of LES simulations that the streamwise spacing of boulders is more important than their spatial density, because of its effect on wake sheltering. Skewness cannot discriminate between different spatial arrangements of the same roughness elements, and ES cannot discriminate between staggered, aligned or random arrays.

What ES can do is allow for directionality; for example, its value would be higher for a step-pool channel than for the same boulders in a flow-aligned arrangement. Directionality can also be important in bedrock rivers flowing over tilted sedimentary or metamorphic strata. Goode & Wohl (2010) used a hydraulic model to calibrate Manning's  $n$  to surveyed water level measurements in different reaches of a sinuous bedrock channel during a steady reservoir release and found that  $n$  was higher in reaches with transverse ribs than in those with oblique or flow-parallel ribs. The ES metric would discriminate between different orientations of a simple corrugated pattern: for a fixed amplitude, ES would vary as the sine of the horizontal angle between the corrugation crest and channel direction.

In rough-bed rivers, one final complication is that bed roughness can change during flood events because of the entrainment, transport and deposition of bed sediment. Most gravel-bed rivers have a coarse surface layer, disruption of which during floods releases finer grains and alters surface roughness. In bedrock rivers, sediment patches may grow or be swept away. In both cases, a roughness height measured in low-flow conditions is likely to misrepresent the effective roughness during the flood event. Topographic metrics like  $\sigma_z$  are affected

by this just as much as grain size metrics like  $D_{84}$ . In extreme floods, there is a further complication: intense sediment transport extracts momentum from the flow and increases the perceived flow resistance (e.g. Recking et al., 2008).

## 7 | DISCUSSION

The literature on estimating open-channel flow resistance from bed roughness metrics rather than grain size is small and inconclusive. The standard deviation of bed elevation,  $\sigma_z$ , is a recognised alternative to  $D_{84}$  but has not consistently been found superior. Drag on immobile boulders has been recognised as important for sediment transport and bedrock incision as well as channel hydraulics, but quantitative calculations depend on insecure assumptions about drag coefficients in shallow flow or calibration of these coefficients by effectively treating them as roughness coefficients.

Given the limited progress that has been made in the fluvial literature, are there lessons to be learnt from the much more extensive literature about rough-surface friction in boundary-layer meteorology and various branches of mechanical and marine engineering? The boundary layers concerned differ from rivers in not having a free surface close to or within the roughness layer, but the near-boundary flow can still be characterised by a log-law roughness height ( $y_0$  or  $k_s$ ) and the literature includes many attempts to correlate this with surface metrics.

One conclusion is that  $\sigma_z$  by itself is a necessary, but not sufficient, predictor of flow resistance over a rough surface. It is a relevant factor because it summarises roughness amplitude, but the engineering literature is unanimous in treating it as only a starting point. The ratio  $k_s/\sigma_z$  is seen as a non-dimensional version of the Nikuradse sand equivalent roughness that is likely to vary with other characteristics of the rough surface. Which metrics are candidates to predict  $k_s/\sigma_z$  depends on whether the surface is regarded as a quasi-random elevation field, as in most of the industrial and naval engineering literature and some fluvial papers, or a finite array of large roughness elements as in other fluvial papers and most of the meteorology literature. In the first perspective (Section 4), the skewness of the elevation distribution is widely seen as important: for a given value of  $\sigma_z$ , a positively-skewed surface with more peaks than pits exerts more drag than its negatively-skewed mirror image. In the obstacle-array perspective (Section 5), the equivalent of skewness is spatial density ( $\lambda_p$ ): low density is associated with positive skewness and either isolated roughness or wake interference, high density with negative skewness and skimming flow. Another aspect of this duality is that the frontal solidity ( $\lambda_f$ ) of an obstacle array is equivalent to the ES metric for a quasi-random surface.

The specific correlations between  $k_s/\sigma_z$  (or  $k_s/k$ ) and skewness and/or other metrics that we discussed and illustrated in Sections 4, 5 and 6 were developed for relatively deep boundary layers and cannot necessarily be expected to hold for shallow open channel flows. Rather, we see them as suggesting metrics, or combinations of metrics, that are worth exploring for use in flow resistance equations for rivers. The leading candidate is skewness ( $\gamma$ ), which is easily computed from a DEM and discriminates between peak-dominated and pit-dominated topography regardless of whether the surface is quasi-random or an obstacle array. In the latter case, it discriminates

between low and high obstacle density. We might therefore expect that using  $\gamma$ , or in some situations boulder density, as well as  $\sigma_z$  could improve predictions of flow resistance in a variety of river types. Effective slope (ES) also looks worth exploring in applications where a DEM or long profile is available, again in combination with  $\sigma_z$  and possibly also  $\gamma$ . ES may be particularly useful in situations where directionality appears relevant.

For rivers with boulder arrays, one question that has received little attention is how to characterise arrays of boulders that differ in size and shape. As we noted in Section 5.3, research by urban meteorologists on mixed-height obstacles appears relevant (e.g. Millward-Hopkins et al., 2011; Xie, Coceal, & Castro, 2008), and sheltering models in general may be relevant to the treatment of friction on the parts of a river bed that are not occupied by boulders.

There are several pointers here for future fluvial research, but also many open questions and research needs. These fall into five groups: (1) the dependence of roughness metrics on how the long profile or DEM is detrended or smoothed; (2) uncertainty about how to quantify the effect of skewness; (3) the choice of what type of flow resistance equation to use; (4) the potential of numerical simulation; and (5) how best to acquire a database of topographic and hydraulic data, which is needed for calibrating and testing proposals.

### 7.1 | Detrending and smoothing

For river beds with quasi-random roughness that can best be characterised statistically, an important open question is how to distinguish between roughness and overall morphology. This is rarely a problem for urban meteorologists and industrial or naval engineers, who are usually concerned with near-planar surfaces with superimposed roughness. Nor is it a problem for flume experiments with plane beds, where all that is necessary is to remove the overall gradient. But the definition of roughness is less obvious in natural river channels with beds that are perceptibly non-planar. As we noted in Section 3.2, if  $\sigma_z$  is regarded as an alternative to  $D_{84}$  as a metric of grain-scale roughness, it is logical to remove any large-scale morphology before computing  $\sigma_z$  from the residual variance in elevation. This, however, risks removing significant sources of flow resistance such as boulder steps or (at least in low-flow conditions) gravel bars. Is it better in such situations to calculate  $\sigma_z$  after doing no more than removing the overall downstream gradient, and hope that by including some larger-scale roughness it can give better predictions of flow resistance than is possible using a grain size?

It is known that the value of  $\sigma_z$  for a particular reach can vary substantially depending on how it is obtained. Is this also the case for other roughness metrics? We speculate that skewness is probably less sensitive and that ES is affected more by DEM resolution than by detrending. Analyses of a range of representative river beds are required to gain information on these potential scale dependencies. Another unknown is whether the effects of smoothing on different metrics have a cumulative influence on predictions of flow resistance or tend to cancel out.

It has become fairly straightforward to obtain high-resolution DEMs of the exposed parts of river channel boundaries using techniques such as terrestrial laser scanning or structure-from-motion photogrammetry. Obtaining data at similar resolution for the

submerged parts of the bed is much more difficult, and in the past involved interpolation from relatively sparse total-station measurements. Topo-bathymetric lidar (e.g. Frizzle et al., 2024; Tonina et al., 2020) is an improvement on this but still has a coarser resolution than above-water methods. That raises the question of how much difference there is between statistical metrics calculated using only the exposed bed at low flow and those calculated for the entire boundary.

## 7.2 | Quantifying the effect of skewness

The consensus view in the literature on obstacle arrays, whether in open-channel flows or the atmospheric boundary layer, is that curves of  $k_s/k$  or  $k_s/\sigma_z$  against spatial density ( $\lambda_p$ ) are asymmetric. Flow resistance is low for very isolated obstacles, increases rapidly to a maximum at a spatial density of roughly 0.2 (Figure 5), then decreases more gradually as obstacle density increases to the high values at which skimming flow prevails. A plot of flow resistance against skewness is asymmetric in the opposite way (Figure 8): low for negative skewness and for very high positive skewness, and greatest at some intermediate positive skewness.

In contrast, there is no consensus in the engineering literature about the effect of skewness on total frictional drag, except that it matters. Researchers in industrial and naval engineering have proposed a variety of correlations between  $k_s/\sigma_z$  and skewness, but they are inconsistent with each other (Figure 4) and with what is implied by obstacle-array models (Figure 9). This may reflect differences in the range of skewness typically encountered in different disciplines and in some cases lack of thought about asymptotic behaviour.

It is therefore unclear what to expect for the effect of skewness on flow resistance in rivers. On the basis of the peaks versus pits through experiment we suspect that positively-skewed roughness is likely to exert more resistance than negatively-skewed roughness of the same amplitude, but in the near-absence of data, it seems premature to propose a functional form for the relation. In boulder-bed channels, it may often be simpler to measure the mean size and spatial density of boulders than to obtain a DEM and compute  $\sigma_z$  and skewness from it. Boulder density then becomes the counterpart of skewness, with low to moderate density corresponding to positive skewness.

## 7.3 | Choice of resistance equation

Not all river beds can realistically be considered as obstacle arrays, but for those boulder-strewn or step-pool channels that can, there is a choice of strategies for estimating flow resistance and thereby predicting mean depth and velocity. What little fluvial research has been done on this has generally taken a stress-partitioning approach (e.g. Yager, Kirchner, & Dietrich, 2007) in which the obstacles and the rest of the bed are treated separately. That approach is obviously appropriate when the interest is in the extent to which shear stress on the rest of the bed is reduced, as in the fluvial research we have cited, but it can also be used to predict overall flow resistance and partition unit discharge between depth and velocity. The boundary-layer meteorology literature is concerned with the same questions,

but some of it tackles the flow-resistance question by deriving an overall log-law  $k_s$  value from the combination of form drag on obstacles and friction on horizontal surfaces, weighted by their different areas and drag coefficients. This is broadly comparable to the use of a single composite roughness height to predict flow resistance in bed-rock rivers with a roughness contrast between sediment and exposed rock (Johnson, 2014) or rock bed and banks (Ferguson, Hardy, & Hodge, 2019).

In river channels with quasi-random roughness, the effects of skewness and/or another metric could be combined with  $\sigma_z$  to generate a single  $k_s$ -like roughness height for use in some existing type of resistance equation. Much of the literature on non-fluvial boundary layers that we have discussed in this review has been directed at predicting a specifically log-law  $k_s$  value, since the boundary layer depth is at least 1 to 2 orders of magnitude higher than the roughness amplitude in most industrial applications and in urban meteorology. In such cases, almost all of the velocity profile is expected to be logarithmic. That is no longer true at low relative submergence in a rough-bed river, so a logarithmic resistance law is not necessarily the best choice.

A roughness height derived from topographic metrics could be used in various non-logarithmic types of resistance equations. One such is  $(8/f)^{1/2} \propto d/k$  which was proposed by Lawrence (1997) and forms the roughness-layer asymptote of the variable-power equation (VPE; Ferguson, 2007). Aberle and Smart (2003), Yochum et al. (2012) and Nitsche et al. (2012) all obtained their best predictions using this relation (or its hydraulic geometry equivalent) with  $k = \sigma_z$ . Nitsche et al. (2012) also found a slight improvement in predictions by making the prefactor of the power law decrease with increasing boulder density; this improvement could equally be achieved by making  $k$  a function of boulder density as well as  $\sigma_z$ . A topography-based roughness height could alternatively be used in the VPE itself, or in either of the VPE-based non-dimensional hydraulic geometry equations proposed by Rickenmann and Recking (2011). These equations do not make explicit use of the friction factor, nor of depth, and instead predict velocity from slope, roughness height and unit discharge. With  $D_{84}$  as the roughness height, Zimmerman (2010) and Rickenmann & Recking (2011) found that prediction errors in velocity were lower in the hydraulic geometry approach than when using a relative-submergence equation, and Chen et al. (2020) found the same with  $\sigma_z$  as the roughness height.

## 7.4 | The potential of numerical simulation

Computational fluid dynamics (CFD) simulations of short reaches of rivers date back to the late 1990s, motivated initially by an interest in large-scale flow structures in confluences and bends. In some cases field measurements were used to specify the water surface and mean inflow velocity in the simulation, thereby making the friction factor part of the model setup. Using CFD to learn about flow resistance requires instead that one or both of depth and velocity is free to vary.

Most of the non-fluvial CFD research discussed in Sections 4 and 6 makes velocity the dependent variable, by simulating flow through a duct with rough upper and lower boundaries. The ratio of duct half height to roughness amplitude (the equivalent of relative submergence in a river) is high enough for almost all of the velocity profile to be logarithmic, allowing  $k_s$  to be estimated from a single simulation. A

logarithmic profile cannot be assumed in a shallow open-channel flow, so the friction factor needs to be determined for a range of depths. This can be achieved in rigid-lid (fixed planar water surface) simulations by varying the driving force at each depth, but in very shallow flows the surface should preferably be free to move up or down to allow irregularities to develop near protruding or just-submerged obstacles. This can be done using the volume-of-fluid method (Hirt & Nichols, 1981), with computation continuing until the free surface has stabilised.

Rather than build a channel gradient into the computational domain it is more convenient to have a horizontal bed with superimposed roughness and drive the flow by a pressure gradient, or in some codes by realigning the gravity vector. Early fluvial applications of CFD used a conventional resistance equation in the basal layer of a curvilinear boundary-fitted mesh, but a more versatile approach is to represent bed roughness using a water/sediment porosity value in the near-basal cells of a rectangular grid (Lane et al., 2004; Olsen & Stokseth, 1995). One technical issue is that Chen et al. (2019) found significantly different results in simulations of a boulder-array reach depending on whether they used a DEM (effectively only 2.5D) or the full structure-from-motion photogrammetry of the field site, including overhangs under the sides of boulders.

CFD simulations are also valuable for learning about the details of flow within the roughness layer. Monsalve, Yager, and Schmeckle (2017) and Zhang et al. (2022) did so using free-surface simulations matched to flume experiments to discover the details of flow around semi-submerged hemispheres, and Chen et al. (2019) made rigid-lid LES simulations of flow over small parts of three field sites. Further work of this kind could give useful insight into the pressure force on protruding boulders, drag coefficients, wave drag and the effect of boulder orientation.

## 7.5 | Data requirements

Calibration and testing of alternative ways to predict flow resistance using  $D_{84}$  have benefited from the abundance of data from all kinds of coarse-bed rivers. Rickenmann and Recking (2011) compiled almost 3,000 field measurements of bulk hydraulics spanning a huge range of slope,  $D_{84}$  and discharge. In contrast, there is very little open-channel flow data for sites at which  $\sigma_z$  is known or topographic data (DEM or other) is publicly available. The only exception we know of is the data compilation of Chen et al. (2020) which is available in the Supplementary Information section of their paper. That compilation is of mid-channel long profiles, not full DEMs, but does include bulk flow data. There may be scope for further analysis of this valuable data set.

Detailed DEMs of coarse alluvial channels and mixed bedrock/alluvial reaches are increasingly available, and one way to start filling the information gap is to make flow measurements at such sites. Measurements would need to be made over a wide range of flow depths since the measured friction factor at one depth might be matched by a predictive relation that is inaccurate at other depths. Field measurements of this type are easier and more reliable at sites close to established gauging stations since reach-averaged depth and velocity can then be obtained just by surveying water surface profiles at different discharges. The sites at which flow data are acquired should be

selected to give a wide range of values of  $\sigma_z$  and other roughness metrics.

There are several other ways to obtain the necessary combination of flow data and topographic data. One is to obtain and analyse bed DEMs of reaches for which bulk flow data are already available and in which there is no evidence of subsequent channel change. Another is to run flume experiments using scaled-down replicas of field sites at which DEMs have been obtained, in the way done by Hodge and Hoey (2016). There is also scope for exploring the effects of one topographic metric at a time in systematically designed programs of flume experiments, going beyond what has already been done for simulated boulder arrays (Section 5.3).

CFD could be used to simulate field prototypes, preferably chosen to have contrasting values of roughness metrics other than  $\sigma_z$ . Free-surface simulations would make it easier to model the effect of changing the water discharge at a given slope, as well as giving more accurate results in very shallow flows in which water surface deformation is expected. There is also great potential in simulating flow over beds with stochastically generated roughness, as in much of the engineering literature that we have discussed in Sections 4 and 6. This could for example allow skewness to be varied while holding  $\sigma_z$  constant or nearly so, allowing results to be generated for a range of relative submergence at each of a range of values of skewness. Likewise, it would be possible to vary one attribute at a time of a boulder array. Another geometric manipulation that might be informative is to add long-wavelength bar-pool-riffle morphology to an initially planar rough bed, to determine the effect on bulk flow resistance at different mean depths.

In summary, despite decades of research, there is still considerable uncertainty in how best to predict the flow resistance of rough-bed rivers. We have demonstrated that work in adjacent fields provides useful suggestions for additional topographic metrics with the potential for improving current approaches. However, further work will also require a database of flow and topographic data to be built up, using a combination of field, flume and CFD methods as outlined above. Given the complexity of the problem and the infinite variety of natural river beds, there may not be any single 'best' method of predicting flow resistance from topographic metrics in rough-bed rivers, but we hope that this review will inspire research using different approaches to the problem.

### NOTATION

$A_f$	frontal area
$C_D$	drag coefficient
$d$	displacement height in log law
$D$	grain diameter
$D_{84}$	84th percentile of grain-size distribution
$ES$	effective slope
$f$	Darcy-Weisbach friction factor
$g$	gravity acceleration
$h$	flow depth
$k$	obstacle height
$k_s$	Nikuradse sand equivalent roughness
$R$	hydraulic radius
$S$	energy slope, channel slope
$u$	mean velocity at a particular height
$u^*$	shear velocity
$v$	mean velocity of stream or river

w	width of square window used in topographic analysis
y	height above bed
$y_0$	zero height in log law
z	bed elevation
$\gamma$	skewness of bed elevation
$\kappa$	von Karman constant
$\lambda_f$	frontal solidity of obstacles
$\lambda_p$	plan density of obstacles
$\rho$	fluid density
$\sigma_z$	standard deviation of bed elevation
$\tau$	total shear stress

## AUTHOR CONTRIBUTIONS

**Conceptualisation:** Robert I. Ferguson. **Investigation:** All. **Analysis:** Robert I. Ferguson, Rebecca A. Hodge and Robert C. Houseago. **Writing—first draft:** Robert C. Houseago and Elowyn M. Yager. **Writing—review and editing:** All.

## ACKNOWLEDGEMENTS

This research was supported by UKRI grant NE/W00125X/1 to Hodge. We thank an associate editor and two anonymous reviewers for comments and suggestions that helped improve the paper.

## CONFLICT OF INTEREST STATEMENT

The authors are not aware of any conflict of interest.

## DATA AVAILABILITY STATEMENT

The data plotted in Figure 3 are available from the corresponding author upon reasonable request. No data were analysed or generated in the rest of the paper.

## ORCID

Robert I. Ferguson  <https://orcid.org/0000-0002-0981-1112>  
 Rebecca A. Hodge  <https://orcid.org/0000-0002-8792-8949>  
 Robert C. Houseago  <https://orcid.org/0000-0001-7646-6489>  
 Elowyn M. Yager  <https://orcid.org/0000-0002-3382-2356>

## REFERENCES

- Abdelaziz, M., Djenidi, L., Ghayesh, M.H. & Chin, R. (2024) On predictive models for the equivalent sand roughness for wall-bounded turbulent flows. *Physics of Fluids*, 36(1), 015125. Available from: <https://doi.org/10.1063/5.0178798>
- Aberle, J. & Nikora, V. (2006) Statistical properties of armored gravel surfaces. *Water Resources Research*, 42(11), W11414. Available from: <https://doi.org/10.1029/2005WR004674>
- Aberle, J. & Smart, G.M. (2003) The influence of roughness structure on flow resistance on steep slopes. *Journal of Hydraulic Research*, 41(3), 259–269. Available from: <https://doi.org/10.1080/00221680309499971>
- Adams, D.L. (2020) Toward bed state morphodynamics in gravel-bed rivers. *Progress in Physical Geography*, 44(5), 700–726. Available from: <https://doi.org/10.1177/0309133320900924>
- Baiamonte, G. & Ferro, V. (1997) The influence of roughness geometry and shields parameter on flow resistance in gravel-bed channels. *Earth Surface Processes and Landforms*, 22(8), 759–772. Available from: [https://doi.org/10.1002/\(SICI\)1096-9837\(199708\)22:8<759::AID-ESP779>3.0.CO;2-M](https://doi.org/10.1002/(SICI)1096-9837(199708)22:8<759::AID-ESP779>3.0.CO;2-M)
- Banke, E.G. & Smith, S.D. (1973) Wind stress on Arctic Sea ice. *Journal of Geophysical Research*, 78(33), 7871–7883. Available from: <https://doi.org/10.1029/JC078i033p07871>
- Barros, J.M., Schultz, M.P. & Flack, K.A. (2018) Measurements of skin friction of systematically generated surface roughness. *International Journal of Heat and Fluid Flow*, 72, 1–7. Available from: <https://doi.org/10.1016/j.ijheatfluidflow.2018.04.015>
- Bathurst, J.C. (1978) Flow resistance of large-scale roughness. *Journal of the Hydraulics Division*, 104(12), 1587–1603. Available from: <https://doi.org/10.1061/JYCEAJ.0005114>
- Bathurst, J.C. (1985) Flow resistance estimation in mountain rivers. *Journal of Hydraulic Engineering*, 111(4), 625–643. Available from: [https://doi.org/10.1061/\(ASCE\)0733-9429\(1985\)111:4\(625\)](https://doi.org/10.1061/(ASCE)0733-9429(1985)111:4(625))
- Bathurst, J.C. (2002) At-a-site variation and minimum flow resistance for mountain rivers. *Journal of Hydrology*, 269(1–2), 11–26. Available from: [https://doi.org/10.1016/S0022-1694\(02\)00191-9](https://doi.org/10.1016/S0022-1694(02)00191-9)
- Bertin, S. & Friedrich, H. (2014) Measurement of gravel-bed topography: evaluation study applying statistical roughness analysis. *Journal of Hydraulic Engineering*, 140(3), 269–279. Available from: [https://doi.org/10.1061/\(ASCE\)HY.1943-7900.0000823](https://doi.org/10.1061/(ASCE)HY.1943-7900.0000823)
- Brasington, J., Vericat, D. & Rychkov, I. (2012) Modeling river bed morphology, roughness, and surface sedimentology using high resolution laser scanning. *Water Resources Research*, 48(11), W11519. Available from: <https://doi.org/10.1029/2012WR012223>
- Bray, D.I. (1980) Evaluation of effective boundary roughness for gravel-bed rivers. *Canadian Journal of Civil Engineering*, 7(2), 392–397. Available from: <https://doi.org/10.1139/l80-047>
- Brayshaw, A.C., Frostick, L.E. & Reid, I. (1983) The hydrodynamics of particle clusters and sediment entrapment in coarse alluvial channels. *Sedimentology*, 30(1), 137–143. Available from: <https://doi.org/10.1111/j.1365-3091.1983.tb00656.x>
- Buechel, M.E.H., Hodge, R.A. & Kenmare, S. (2022) The influence of bedrock river morphology and alluvial cover on gravel entrainment: part 1. Pivot angles and surface roughness. *Earth Surface Processes and Landforms*, 47(14), 3361–3375. Available from: <https://doi.org/10.1002/esp.5463>
- Busse, A. & Jelly, T.O. (2023) Effect of high skewness and kurtosis on turbulent channel flow over irregular rough walls. *Journal of Turbulence*, 24(1–2), 57–81. Available from: <https://doi.org/10.1080/14685248.2023.2173761>
- Butler, J.B., Lane, S.N. & Chandler, J.H. (1998) Assessment of DEM quality for characterizing surface roughness using close range digital photogrammetry. *Photogrammetric Record*, 16(92), 271–291. Available from: <https://doi.org/10.1111/0031-868X.00126>
- Canovaro, F., Paris, E. & Solari, F. (2007) Effects of macro-scale bed roughness geometry on flow resistance. *Water Resources Research*, 43(10), W10414. Available from: <https://doi.org/10.1029/2006WR005727>
- Chen, X., Hassan, M.A., An, C. & Fu, X. (2020) Rough correlations: meta-analysis of roughness measures in gravel-bed rivers. *Water Resources Research*, 56(8), e2020WR027079. Available from: <https://doi.org/10.1029/2020WR027079>
- Chen, Y., DiBiase, R.A., McCarroll, N. & Liu, X. (2019) Quantifying flow resistance in mountain streams using computational fluid dynamics modeling over structure-from-motion photogrammetry-derived microtopography. *Earth Surface Processes and Landforms*, 44(10), 1973–1987. Available from: <https://doi.org/10.1002/esp.4624>
- Chung, D., Hutchins, N., Schultz, M.P. & Flack, K.A. (2021) Predicting the drag of rough surfaces. *Annual Review of Fluid Mechanics*, 53(1), 439–471. Available from: <https://doi.org/10.1146/annurev-fluid-062520-115127>
- Church, M., Hassan, M.A. & Wolcott, J.F. (1998) Stabilizing self-organized structures in gravel-bed stream channels: field and experimental observations. *Water Resources Research*, 34(11), 3169–3179. Available from: <https://doi.org/10.1029/98WR00484>
- Deal, E. (2022) Flow resistance in very rough channels. *Water Resources Research*, 58(10), e2021WR031790. Available from: <https://doi.org/10.1029/2021WR031790>
- Ergenzinger, P. (1992) Riverbed adjustments in a step-pool system: Lainbach, Upper Bavaria. In: Billi, P., Hey, R.D., Thorne, C.R. & Tacconi, P. (Eds.) *Dynamics of gravel-bed rivers*. Chichester: Wiley, pp. 415–430.
- Fang, H.W., Liu, Y. & Stoesser, T. (2017) Influence of boulder concentration on turbulence and sediment transport in open-channel flow over submerged boulders. *Journal of Geophysical Research - Earth Surface*, 122(12), 2392–2410. Available from: <https://doi.org/10.1002/2017JF004221>

- Ferguson, R. (2007) Flow resistance equations for gravel- and boulder-bed streams. *Water Resources Research*, 43(5), W05427. Available from: <https://doi.org/10.1029/2006WR005422>
- Ferguson, R.I. (2022) Reach-scale flow resistance. In: Shroder, J.J.F. (Ed.) *Treatise on geomorphology*, Vol. 6. San Diego: Elsevier, Academic Press, pp. 110–132 <https://doi.org/10.1016/B978-0-12-409548-9.09386-6>
- Ferguson, R.I., Hardy, R.J. & Hodge, R.A. (2019) Flow resistance and hydraulic geometry in bedrock rivers with multiple roughness length scales. *Earth Surface Processes and Landforms*, 44(12), 2437–2449. Available from: <https://doi.org/10.1002/esp.4673>
- Ferguson, R.I., Sharma, B.P., Hodge, R.A., Hardy, R.J. & Warburton, J. (2017) Flow resistance and hydraulic geometry in contrasting reaches of a bedrock channel. *Water Resources Research*, 53(3), 2278–2293. Available from: <https://doi.org/10.1002/2016WR020233>
- Ferro, V. & Giordano, G. (1991) Experimental study of flow resistance in gravel-bed rivers. *Journal of Hydraulic Engineering*, 117(10), 1239–1246. Available from: [https://doi.org/10.1061/\(ASCE\)0733-9429\(1991\)117:10\(1239\)](https://doi.org/10.1061/(ASCE)0733-9429(1991)117:10(1239))
- Finnegan, N.J., Sklar, L.S. & Fuller, T.K. (2007) Interplay of sediment supply, river incision, and channel morphology revealed by the transient evolution of an experimental bedrock channel. *Journal of Geophysical Research - Earth Surface*, 112(F3), F03S11. Available from: <https://doi.org/10.1029/2006JF000569>
- Flack, K.A. & Schultz, M.P. (2010) Review of hydraulic roughness scales in the fully rough regime. *Journal of Fluids Engineering*, 132(4), 041203. Available from: <https://doi.org/10.1115/1.4001492>
- Flack, K.A., Schultz, M.P. & Barros, J.M. (2020) Skin friction measurements of systematically-varied roughness: probing the role of roughness amplitude and skewness. *Flow, Turbulence and Combustion*, 104(2–3), 317–329. Available from: <https://doi.org/10.1007/s10494-019-00077-1>
- Flammer, G.H., Tullis, J.P. & Mason, E.S. (1970) Free surface, velocity gradient flow past hemisphere. *Journal of the Hydraulics Division*, 96(7), 1485–1502. Available from: <https://doi.org/10.1061/JYCEAJ.0002563>
- Fonstad, M.A., Dietrich, J.T., Courville, B.C., Jensen, J.L. & Carbonneau, P.E. (2013) Topographic structure from motion: a new development in photogrammetric measurement. *Earth Surface Processes and Landforms*, 38(4), 421–430. Available from: <https://doi.org/10.1002/esp.3366>
- Forooghi, P., Stroh, A., Magagnato, F., Jakirlic, S. & Frohnapfel, B. (2017) Toward a universal roughness correlation. *Journal of Fluids Engineering*, 139(12), 121201. Available from: <https://doi.org/10.1115/1.4037280>
- Frizzle, C., Trudel, M., Daniel, S., Pruneau, A. & Noman, J. (2024) LiDAR topo-bathymetry for riverbed elevation assessment: a review of approaches and performance for hydrodynamic modelling of floodplains. *Earth Surface Processes and Landforms*, 49(9), 2585–2600. Available from: <https://doi.org/10.1002/esp.5808>
- Furbish, D.J. (1987) Conditions for geometric similarity of coarse streambed roughness. *Mathematical Geology*, 19(4), 291–307. Available from: <https://doi.org/10.1007/BF00897840>
- Gomez, B. (1993) Roughness of stable, armoured river beds. *Water Resources Research*, 29(11), 3631–3642. Available from: <https://doi.org/10.1029/93WR01490>
- Goode, J.R. & Wohl, E. (2010) Substrate controls on the longitudinal profile of bedrock channels: implications for reach-scale roughness. *Journal of Geophysical Research*, 115(F3), F03018. Available from: <https://doi.org/10.1029/2008JF001188>
- Griffiths, G.A. (1981) Flow resistance in coarse gravel bed rivers. *Journal of the Hydraulics Division*, 107(7), 899–918. Available from: <https://doi.org/10.1061/JYCEAJ.0005699>
- Grimmond, C.S.B. & Oke, T.R. (1999) Aerodynamic properties of urban areas derived from analysis of surface form. *Journal of Applied Meteorology*, 38(9), 1262–1292. Available from: [https://doi.org/10.1175/1520-0450\(1999\)038<1262:APOUAD>2.0.CO;2](https://doi.org/10.1175/1520-0450(1999)038<1262:APOUAD>2.0.CO;2)
- Hama, F.R. (1954) Boundary-layer characteristics for smooth and rough surfaces. *Transactions of the Society of Naval Architects and Marine Engineers*, 62, 333–358.
- Hassan, M.A. & Reid, I. (1990) The influence of microform bed roughness elements on flow and sediment transport in gravel bed rivers. *Earth Surface Processes and Landforms*, 15(8), 739–750. Available from: <https://doi.org/10.1002/esp.3290150807>
- Herbich, J. & Shulits, S. (1964) Large-scale roughness in open-channel flow. *Journal of Hydraulics Division*, ASCE, 90(6), 203–230. Available from: <https://doi.org/10.1061/JYCEAJ.0001133>
- Heritage, G.L. & Milan, D.J. (2009) Terrestrial laser scanning of grain roughness in a gravel-bed river. *Geomorphology*, 113(1–2), 4–11. Available from: <https://doi.org/10.1016/j.geomorph.2009.03.021>
- Hey, R.D. (1979) Flow resistance in gravel-bed rivers. *Journal of the Hydraulics Division*, 105(4), 365–379. Available from: <https://doi.org/10.1061/JYCEAJ.0005178>
- Hirt, C.W. & Nichols, B.D. (1981) Volume of fluid (VoF) method for the dynamics of free boundaries. *Journal of Computational Physics*, 39(1), 201–225. Available from: [https://doi.org/10.1016/0021-9991\(81\)90145-5](https://doi.org/10.1016/0021-9991(81)90145-5)
- Hodge, R., Brasington, J. & Richards, K. (2009) In situ characterization of grain-scale fluvial morphology using terrestrial laser scanning. *Earth Surface Processes and Landforms*, 34(7), 954–968. Available from: <https://doi.org/10.1002/esp.1780>
- Hodge, R.A. & Hoey, T.B. (2016) A Froude-scaled model of a bedrock-alluvial channel reach: 1. Hydraulics. *Journal of Geophysical Research: Earth Surface*, 121(9), 1578–1596. Available from: <https://doi.org/10.1002/2015JF003706>
- Houseago, R., Hodge, R., Ferguson, R., Hardy, R., Hackney, C., Rice, S., Johnson, J., Yager, E., Hoey, T., & Yamasaki, T. (2024). Surface roughness: capturing rough-bed river diversity. Available from: <https://doi.org/10.5194/egusphere-egu24-11154>
- Iseya, F. & Ikeda, H. (1987) Pulsations in bedload transport rates induced by a longitudinal sediment sorting: a flume study using sand and gravel mixtures. *Geografiska Annaler*, 69A(1), 15–27. Available from: <https://doi.org/10.1080/04353676.1987.11880193>
- Johnson, J.P.L. (2014) A surface roughness model for predicting alluvial cover and bed load transport rate in bedrock channels. *Journal of Geophysical Research - Earth Surface*, 119(10), 2147–2173. Available from: <https://doi.org/10.1002/2013JF003000>
- Jouybari, M.A., Yuan, J., Brereton, G.J. & Murillo, M.S. (2021) Data-driven prediction of the equivalent sand-grain height in rough-wall turbulent flows. *Journal of Fluid Mechanics*, 912, A8. Available from: <https://doi.org/10.1017/jfm.2020.1085>
- Judd HE, Peterson DF (1969) Hydraulics of large bed element channels. *Utah Water Research Laboratory rept. PRWG 17-6*, 85 pp.
- Keulegan, G.H. (1938) Laws of turbulent flow in open channels. *Journal of Research of the National Bureau of Standards*, 21(6), 707–741. Available from: <https://doi.org/10.6028/jres.021.039>
- Kuipers, H. (1957) A relief meter for soil cultivation studies. *Netherlands Journal of Agricultural Science*, 5, 255–262.
- Lamb, M.P. & Brun, F. (2017) Direct measurements of lift and drag on shallowly submerged cobbles in steep streams: implications for flow resistance and sediment transport. *Water Resources Research*, 53(9), 7607–7629. Available from: <https://doi.org/10.1002/2017WR020883>
- Lamb, M.P., Brun, F. & Fuller, B.M. (2017) Hydrodynamics of steep streams with planar coarse-grained beds: turbulence, flow resistance, and implications for sediment transport. *Water Resources Research*, 53(3), 2240–2263. Available from: <https://doi.org/10.1002/2016WR019579>
- Lane, S.N. (2005) Roughness – time for a re-evaluation. *Earth Surface Processes and Landforms*, 30(2), 251–253. Available from: <https://doi.org/10.1002/esp.1208>
- Lane, S.N., Hardy, R.J., Elliott, L. & Ingham, D.B. (2004) Numerical modeling of flow processes over gravelly surfaces using structured grids and a numerical porosity scheme. *Water Resources Research*, 40(1), W01302. Available from: <https://doi.org/10.1029/2002WR001934>
- Lawrence, D.S.L. (1997) Macroscale surface roughness and frictional resistance in overland flow. *Earth Surface Processes and Landforms*, 22(4), 365–382. Available from: [https://doi.org/10.1002/\(SICI\)1096-9837\(199704\)22:4<365::AID-ESP693>3.0.CO;2-6](https://doi.org/10.1002/(SICI)1096-9837(199704)22:4<365::AID-ESP693>3.0.CO;2-6)

- Lawrence, D.S.L. (2000) Hydraulic resistance in overland flow during partial and marginal surface inundation: experimental observations and modeling. *Water Resources Research*, 36(8), 2381–2393. Available from: <https://doi.org/10.1029/2000WR900095>
- Macdonald, R.W., Griffiths, R.F. & Hall, D.J. (1998) An improved method for the estimation of surface roughness of obstacle arrays. *Atmospheric Environment*, 32(11), 1857–1864. Available from: [https://doi.org/10.1016/S1352-2310\(97\)00403-2](https://doi.org/10.1016/S1352-2310(97)00403-2)
- Manga, M. & Kirchner, J.W. (2000) Stress partitioning in streams by large woody debris. *Water Resources Research*, 36(8), 2373–2379. Available from: <https://doi.org/10.1029/2000WR900153>
- Millward-Hopkins, J.T., Tomlin, A.S., Ma, L., Ingham, D. & Pourkashanian, M. (2011) Estimating aerodynamic parameters of urban-like surfaces with heterogeneous building heights. *Boundary-Layer Meteorology*, 141(3), 443–465. Available from: <https://doi.org/10.1007/s10546-011-9640-2>
- Monsalve, A., Yager, E.M. & Schmeeckle, M.W. (2017) Effects of bed forms and large protruding grains on near-bed flow hydraulics in low relative submergence conditions. *Journal of Geophysical Research - Earth Surface*, 122(10), 1845–1866. Available from: <https://doi.org/10.1002/2016JF004152>
- Morris, H.M. (1955) A new concept of flow in rough conduits. *Transactions. American Society of Civil Engineers*, 120(1), 373–398. Available from: <https://doi.org/10.1061/TACEAT.0007206>
- Napoli, E., Armenio, V. & De Marchis, M. (2008) The effect of the slope of irregularly distributed roughness elements on turbulent wall-bounded flows. *Journal of Fluid Mechanics*, 613, 385–394. Available from: <https://doi.org/10.1017/S0022112008003571>
- Nepf, H.M. (1999) Drag, turbulence, and diffusion in flow through emergent vegetation. *Water Resources Research*, 35(2), 479–489. Available from: <https://doi.org/10.1029/1998WR900069>
- Nikora, V., Goring, D., McEwan, I. & Griffiths, G. (2001) Spatially averaged flow over rough bed. *Journal of Hydraulic Engineering*, 127(2), 123–133. Available from: [https://doi.org/10.1061/\(ASCE\)0733-9429\(2001\)127:2\(123\)](https://doi.org/10.1061/(ASCE)0733-9429(2001)127:2(123))
- Nikora, V., Koll, K., McEwan, I., McLean, S. & Ditttrich, A. (2004) Velocity distribution in the roughness layer of rough-bed flows. *Journal of Hydraulic Engineering*, 130(10), 1036–1042. Available from: [https://doi.org/10.1061/\(ASCE\)0733-9429\(2004\)130:10\(1036\)](https://doi.org/10.1061/(ASCE)0733-9429(2004)130:10(1036))
- Nikora, V., McEwan, I., McLean, S., Coleman, S., Pokrajac, D. & Walters, R. (2007) Double-averaging concept for rough-bed open-channel and overland flows: theoretical background. *Journal of Hydraulic Engineering*, 133(8), 873–883. Available from: [https://doi.org/10.1061/\(ASCE\)0733-9429\(2007\)133:8\(873\)](https://doi.org/10.1061/(ASCE)0733-9429(2007)133:8(873))
- Nikora, V. & Walsh, J. (2004) Water-worked gravel surfaces high-order structure functions at the particle scale. *Water Resources Research*, 40(12), W12601. Available from: <https://doi.org/10.1029/2004WR003346>
- Nikora, V.I., Goring, D.G. & Biggs, B.J.F. (1998) On gravel-bed roughness characterization. *Water Resources Research*, 34(3), 517–527. Available from: <https://doi.org/10.1029/97WR02886>
- Nikuradse, J. (1933) Strömungsgesetze in rauhen Röhren. *VDI Forschungsheft*, 361, 1–22.
- Nitsche, M., Rickenmann, D., Kirchner, J.W., Turowski, J.M. & Badoux, A. (2012) Macroroughness and variations in reach-averaged flow resistance in steep mountain streams. *Water Resources Research*, 48(12), W12518. Available from: <https://doi.org/10.1029/2012WR012091>
- Nowell, A.R.M. & Church, M. (1979) Turbulent flow in a depth-limited boundary layer. *Journal of Geophysical Research*, 84(C8), 4816–4823. Available from: <https://doi.org/10.1029/JC084iC08p04816>
- Olsen, N.R.B. & Stokseth, S. (1995) Three-dimensional numerical modelling of water flow in a river with large bed roughness. *Journal of Hydraulic Research*, 33(4), 571–581. Available from: <https://doi.org/10.1080/00221689509498662>
- Parker, G. (1991) Selective sorting and abrasion of river gravels, I: theory. *Journal of Hydraulic Engineering*, 117(2), 131–149. Available from: [https://doi.org/10.1061/\(ASCE\)0733-9429\(1991\)117:2\(131\)](https://doi.org/10.1061/(ASCE)0733-9429(1991)117:2(131))
- Parker, G. & Peterson, A.W. (1980) Bar resistance of gravel-bed streams. *Journal of the Hydraulics Division*, 106(10), 1559–1575. Available from: <https://doi.org/10.1061/JYCEAJ.0005529>
- Pearson, E., Smith, M.W., Klaar, M.J. & Brown, L.E. (2017) Can high resolution 3D topographic surveys provide reliable grain size estimates in gravel bed rivers? *Geomorphology*, 293, 143–155. Available from: <https://doi.org/10.1016/j.geomorph.2017.05.015>
- Penna, N., Padhi, E., Dey, S. & Gaudio, R. (2021) Statistical characterization of unworked and water-worked gravel-bed roughness structures. *Journal of Hydraulic Research*, 3(3), 420–436. Available from: <https://doi.org/10.1080/00221686.2020.1780496>
- Polvi, L.E. (2021) Morphodynamics of boulder-bed semi-alluvial streams in northern Fennoscandia: a flume experiment to determine sediment self-organization. *Water Resources Research*, 57(3), e2020WR028859. Available from: <https://doi.org/10.1029/2020WR028859>
- Powell, D.M. (2014) Flow resistance in gravel-bed rivers: progress in research. *Earth-Science Reviews*, 136, 301–338. Available from: <https://doi.org/10.1016/j.earscirev.2014.06.001>
- Powell, D.M., Ockelford, A., Rice, S.P., Hillier, J.K., Nguyen, T., Reid, I., et al. (2016) Structural properties of mobile armors formed at different flow strengths in gravel-bed rivers. *Journal of Geophysical Research - Earth Surface*, 121(8), 1494–1515. Available from: <https://doi.org/10.1002/2015JF003794>
- Raupach, M.R. (1992) Drag and drag partition on rough surfaces. *Boundary-Layer Meteorology*, 60(4), 375–395. Available from: <https://doi.org/10.1007/BF00155203>
- Raupach, M.R. & Shaw, R.H. (1982) Averaging procedures for flow within vegetation canopies. *Boundary-Layer Meteorology*, 22(1), 79–90. Available from: <https://doi.org/10.1007/BF00128057>
- Raupach, M.R., Thom, A.S. & Edwards, I. (1980) A wind tunnel study of turbulent flow close to regularly arrayed rough surfaces. *Boundary-Layer Meteorology*, 18(4), 373–397. Available from: <https://doi.org/10.1007/BF00119495>
- Recking, A., Frey, P., Paquier, A., Belleudy, P. & Champagne, J.Y. (2008) Feedback between bed load transport and flow resistance in gravel and cobble bed rivers. *Water Resources Research*, 44(5), W05412. Available from: <https://doi.org/10.1029/2007WR006219>
- Rickenmann, D. (1991) Hyperconcentrated flow and sediment transport at steep slopes. *Journal of Hydraulic Engineering*, 117(11), 1419–1439. Available from: [https://doi.org/10.1061/\(ASCE\)0733-9429\(1991\)117:11\(1419\)](https://doi.org/10.1061/(ASCE)0733-9429(1991)117:11(1419))
- Rickenmann, D.A. & Recking, A. (2011) Evaluation of flow resistance equations using a large field data base. *Water Resources Research*, 47, W07538.
- Robert, A. (1988) Statistical properties of sediment bed profiles in alluvial channels. *Mathematical Geology*, 20(3), 205–225. Available from: <https://doi.org/10.1007/BF00890254>
- Roughness Database. (n.d.) (<https://roughnessdatabase.org>, accessed 24 March 2024).
- Sarakinos, S. & Busse, A. (2022) Investigation of rough-wall turbulence over barnacle roughness with increasing solidity using direct numerical simulations. *Physical Review Fluids*, 7(6), 064602. Available from: <https://doi.org/10.1103/PhysRevFluids.7.064602>
- Schlichting, H. (1936) Experimentelle untersuchungen zum rauhgigkeitsproblem. *Ingenieur Archiv*, 7(1), 1–34. Available from: <https://doi.org/10.1007/BF02084166>
- Schmeeckle, M.W., Nelson, J.M. & Shreve, R.L. (2007) Forces on stationary particles in near-bed turbulent flows. *Journal of Geophysical Research - Earth Surface*, 112(F2), F02003. Available from: <https://doi.org/10.1029/2006JF000536>
- Schneider, J.M., Rickenmann, D., Turowski, J.M. & Kirchner, J.W. (2015) Self-adjustment of stream bed roughness and flow velocity in a steep mountain channel. *Water Resources Research*, 51(10), 7838–7859. Available from: <https://doi.org/10.1002/2015WR016934>
- Shao, Y. & Yang, Y. (2005) A scheme for drag partition over rough surfaces. *Atmospheric Environment*, 39(38), 7351–7361. Available from: <https://doi.org/10.1016/j.atmosenv.2005.09.014>
- Shao, Y. & Yang, Y. (2008) A theory for drag partition over rough surfaces. *Journal of Geophysical Research - Earth Surface*, 113, F02805.
- Shobe, C.M., Tucker, G.E. & Anderson, R.S. (2016) Hillslope-derived blocks retard river incision. *Geophysical Research Letters*, 43(10), 5070–5078. Available from: <https://doi.org/10.1002/2016GL069262>

- Smart, G., Aberle, J., Duncan, M. & Walsh, J. (2004) Measurement and analysis of alluvial bed roughness. *Journal of Hydraulic Research*, 42(3), 227–237. Available from: <https://doi.org/10.1080/00221686.2004.9728388>
- Smart, G.M., Duncan, M.J. & Walsh, J.M. (2002) Relatively rough flow resistance equations. *Journal of Hydraulic Engineering*, 128(6), 568–578. Available from: [https://doi.org/10.1061/\(ASCE\)0733-9429\(2002\)128:6\(568\)](https://doi.org/10.1061/(ASCE)0733-9429(2002)128:6(568))
- Smith, M.W. (2014) Roughness in the earth sciences. *Earth-Science Reviews*, 136, 202–225. Available from: <https://doi.org/10.1016/j.earscirev.2014.05.016>
- Thappeta, S.K., Bhallamudi, S.M., Fiener, P. & Narasimhan, B. (2017) Resistance in steep open channels due to randomly distributed macroroughness elements at large Froude numbers. *Journal of Hydrologic Engineering*, 22(12), 04017052. Available from: [https://doi.org/10.1061/\(ASCE\)HE.1943-5584.0001587](https://doi.org/10.1061/(ASCE)HE.1943-5584.0001587)
- Tonina, D. & Buffington, J.M. (2007) Hyporheic exchange in gravel bed rivers with pool-riffle morphology: laboratory experiments and three-dimensional modeling. *Water Resources Research*, 43(1), W01421. Available from: <https://doi.org/10.1029/2005WR004328>
- Tonina, D., McKean, J.A., Benjankar, R.M., Yager, E., Carmichael, R.A., Chen, Q., et al. (2020) Evaluating the performance of topobathymetric LiDAR to support multi-dimensional flow modelling in a gravel-bed mountain stream. *Earth Surface Processes and Landforms*, 45(12), 2850–2868. Available from: <https://doi.org/10.1002/esp.4934>
- Vazquez-Tarrio, D., Borgniet, L., Liebault, F. & Recking, A. (2017) Using UAS optical imagery and SfM photogrammetry to characterize the surface grain size of gravel bars in a braided river (Vénéon River, French Alps). *Geomorphology*, 285, 94–105. Available from: <https://doi.org/10.1016/j.geomorph.2017.01.039>
- Westoby, M.J., Brasington, J., Glasser, N.F., Hambrey, M.J. & Reynolds, J.M. (2012) ‘Structure-from motion’ photogrammetry: a low-cost, effective tool for geoscience applications. *Geomorphology*, 179, 300–314. Available from: <https://doi.org/10.1016/j.geomorph.2012.08.021>
- Wiberg, P.L. & Smith, J.D. (1991) Velocity distribution and bed roughness in high-gradient streams. *Water Resources Research*, 27(5), 825–838. Available from: <https://doi.org/10.1029/90WR02770>
- Wiener, J.S. & Pasternak, G.B. (2022) Scale dependent spatial structuring of mountain river large bed elements maximises flow resistance. *Geomorphology*, 416, 108431. Available from: <https://doi.org/10.1016/j.geomorph.2022.108431>
- Woodget, A.S., Fyffe, C. & Carboneau, P.E. (2018) From manned to unmanned aircraft: adapting airborne particle size mapping methodologies to the characteristics of sUAS and SfM. *Earth Surface Processes and Landforms*, 43(4), 857–870. Available from: <https://doi.org/10.1002/esp.4285>
- Xie, Z.-T., Coceal, O. & Castro, I.P. (2008) Large-eddy simulation of flows over random urban-like obstacles. *Boundary-Layer Meteorology*, 129(1), 1–23. Available from: <https://doi.org/10.1007/s10546-008-9290-1>
- Yager, E.M., Dietrich, W.E., Kirchner, J.W. & McArdeell, B.W. (2012a) Patch dynamics and stability in steep, rough streams. *Journal of Geophysical Research - Earth Surface*, 117(F2), F02010. Available from: <https://doi.org/10.1029/2011JF002253>
- Yager, E.M., Kirchner, J.W. & Dietrich, W.E. (2007) Calculating bed load transport in steep boulder bed channels. *Water Resources Research*, 43(7), W07418. Available from: <https://doi.org/10.1029/2006WR005432>
- Yager, E.M., Turowski, J.M., Rickenmann, D. & McArdeell, B.W. (2012b) Sediment supply, grain protrusion, and bedload transport in mountain streams. *Geophysical Research Letters*, 39(10), L10402. Available from: <https://doi.org/10.1029/2012GL051654>
- Yang, X.I.A., Sadique, J., Mittal, R. & Meneveau, C. (2016) Exponential roughness layer and analytical model for turbulent boundary layer flow over rectangular-prism roughness elements. *Journal of Fluid Mechanics*, 789, 127–165. Available from: <https://doi.org/10.1017/jfm.2015.687>
- Yang, X.I.A., Zhang, W., Yuan, J. & Kunz, R.F. (2023) In search of a universal rough wall model. *Journal of Fluids Engineering*, 145(10), 101302. Available from: <https://doi.org/10.1115/1.4062820>
- Yochum, S.E., Bledsoe, B.P., David, G.C.L. & Wohl, E. (2012) Velocity prediction in high-gradient channels. *Journal of Hydrology*, 424, 84–98. Available from: <https://doi.org/10.1016/j.jhydrol.2011.12.031>
- Zhang, C., Xu, Y., Hassan, M.A., Xu, M. & He, P. (2022) A combined approach of experimental and numerical modeling for 3D hydraulic features of a step-pool unit. *Earth Surface Dynamics*, 110(6), 1253–1272. Available from: <https://doi.org/10.5194/esurf-10-1253-2022>
- Zimmerman, A. (2010) Flow resistance in steep streams: an experimental study. *Water Resources Research*, 46(9), W09536. Available from: <https://doi.org/10.1029/2009WR007913>

**How to cite this article:** Ferguson, R.I., Hardy, R.J., Hodge, R.A., Houseago, R.C., Yager, E.M. & Yamasaki, T.N. (2024) Predicting flow resistance in rough-bed rivers from topographic roughness: Review and open questions. *Earth Surface Processes and Landforms*, 1–20. Available from: <https://doi.org/10.1002/esp.6016>